# Manganese-Mediated Synthesis of a NHC Core Non-Symmetric Pincer Ligand and Evaluation of Its Coordination Properties

Dmitry A. Valyaev,[†,*] Jérémy Willot,[†] Loïc P. Mangin,[‡] Davit Zargarian,[‡] Noël Lugan[†,*]

[†] LCC-CNRS, Université de Toulouse, INPT, UPS, 205 route de Narbonne 31077 Toulouse Cedex 4, France

[‡] Département de Chimie, Université de Montréal, Montréal, Québec H3C 3J7, Canada

# Electronic Supplementary Information

## Table of contents

## Experimental details

**General information.** All manipulations were carried out using Schlenk techniques under an atmosphere of dry nitrogen. Dry and oxygen-free organic solvents (THF, $Et_2O$, $CH_2Cl_2$, toluene, pentane) were obtained using LabSolv (Innovative Technology) solvent purification system. Acetonitrile was dried over $P_2O_5$ and distilled under argon prior to use. Hexane, toluene, THF and $CH_2Cl_2$ used for column chromatography purification were deoxygenated by nitrogen bubbling during 15-20 min. Deuterated chloroform used for NMR spectroscopy was filtered through a short column of basic alumina, degassed by three freeze-pump-thaw cycles and stored over molecular sieves (4Å). Other deuterated solvents ($C_6D_6$, THF-$d_8$, $CD_2Cl_2$, $(CD_3)_2CO$) were degassed by three freeze-pump-thaw cycles and stored over molecular sieves (4Å). Manganese methylenephosphonium complex [$Cp(CO)_2Mn(\eta^2$-$Ph_2P{=}C(H)Ph)]BF_4$ ([**1**]$BF_4$),[S1] *N*-(2-pyridyl)imidazole,[S2] $[Rh(cod)Cl]_2$,[S3] $[NiBr_2(NC$*i*-$Pr)]_n$,[S4] were prepared according to previously described procedures. All other reagent grade chemicals purchased from commercial sources were used as received. A liquid nitrogen/ethanol slush bath was used to maintain samples at the desired low temperature. Photochemical demetallation of [**2**]$BF_4$ was performed in 125 mL reactor with an immersed 150 W Hg medium pressure lamp cooled by Pyrex jacket with circulating water. Chromatographic purification of the compounds was performed on silica (0.060-0.200 mm, 60 Å) obtained from Acros Organics flushed with nitrogen just before use.

Solution IR spectra were recorded in 0.1 mm $CaF_2$ cells using a Perkin Elmer Frontier FT-IR spectrometer and given in $cm^{-1}$ with relative intensity in parentheses. $^1H$, $^{31}P$, and $^{13}C$ NMR spectra were obtained on Bruker Avance 400, Avance III HD 400 or Avance 500 spectrometers and referenced to the residual signals of deuterated solvent[S5] ($^1H$ and $^{13}C$) and to 85% $H_3PO_4$ ($^{31}P$ external standard). When necessary the additional information on the carbon signals attribution was obtained using $^{13}C\{^1H,^{31}P\}$, J-modulated spin-echo (JMOD) $^{13}C\{^1H\}$, and $^1H$–$^{13}C$ HMQC experiments. Mass spectra (ESI mode) were obtained using Thermo Scientific LCQ Fleet instrument. Elemental analysis was carried out in LCC du CNRS (Toulouse, France) and University of Montreal (Montreal, Canada) using Perkin Elmer 2400 series II, and EAS1108, Fisons instruments S.p.A. analyzers, respectively.

**Synthesis of imidazolium salt [3·H]$BF_4$.** *N*-(2-pyridyl)imidazole (305 mg, 2.1 mmol) was added as a solid to a solution of [**1**]$BF_4\times0.25CH_2Cl_2$ (1.12 g, 2 mmol) in $CH_2Cl_2$ (20 mL) at r.t. The color of the solution changed from orange to yellow and the formation of the corresponding manganese phosphine complex [**2**]$BF_4$ as only product was evidenced by IR monitoring and NMR spectrum of a reaction aliquot in $CDCl_3$. The resulting solution was transferred to a photochemical reactor, diluted with $CH_2Cl_2$ (*ca.* 100 mL) and irradiated with visible light under vigorous stirring at room temperature until CO evolution ceased (*ca.* 15 min). The resulting suspension was filtered through Celite and the filter cake was washed with $CH_2Cl_2$ (20 mL). Then degassed saturated aqueous solution of $NaHCO_3$ (5 mL) was added to the solution and the mixture was vigorously shaken until $CO_2$ evolution ceased. All volatiles were evaporated under vacuum and the crude product was purified by column chromatography on silica (3×7 cm). Elution with $CH_2Cl_2$ containing 1% vol. of

$Et_3N$ afforded a light yellow band containing some polymeric impurities (discarded), followed by large yellow band of the target product [**3**·H]$BF_4$, which was eluted with a 99:1:1 $CH_2Cl_2$/MeOH/$Et_3N$ mixture. The eluate was evaporated under vacuum and dissolved in THF (15-20 mL). The solution was filtered through Celite, evaporated to dryness and thoroughly dried under vacuum to give [**3**·H]$BF_4$ (782 mg, 73%) reproducibly containing *ca.* 0.4 molecule of THF according to NMR and elemental microanalysis.

[**2**]$BF_4$: $^1$H NMR (400.1 MHz, $CDCl_3$, 25 °C): δ 9.51 (s, 1H, C*H*$_{Im\text{-}2}$), 8.45 (d, $^3J_{HH}$ = 4.4 Hz, 1H, Py), 8.09 (s, 1H, C*H*$_{Im\text{-}4,5}$), 8.02–7.91 (m, 2H, Ph), 7.63–7.53 (m, 4H, Ph + Py), 7.50–7.41 (m, 7H, Ph + Py), 7.36–7.28 (m, 5H, Ph), 7.23 (s, 1H, C*H*$_{Im\text{-}4,5}$), 6.92 (d, $^2J_{PH}$ = 3.4 Hz, 1H, C*H*Ph), 4.19 (d, $J_{PH}$ = 1.6 Hz, 5H, Cp). $^{31}$P{$^1$H} NMR (162.0 MHz, $CDCl_3$, 25 °C): δ 112.7 (br s). IR ($CH_2Cl_2$): $\nu_{CO}$ 1938.0 (s), 1871.0 cm$^{-1}$ (s), $\nu_{C=C}$ 1601.5 (w), 1538.0 (w) cm$^{-1}$.

[**3**·H]$BF_4$×0.4THF: $^1$H NMR (400.1 MHz, $CDCl_3$, 25 °C): δ 9.40 (s, 1H, C*H*$_{Im\text{-}2}$), 8.43 (d, $^3J_{HH}$ = 4.7 Hz, 1H, Py), 8.12 (s, 1H, C*H*$_{Im\text{-}4,5}$), 7.90 (t, $^3J_{HH}$ = 7.8 Hz, 2H, Ph), 7.84 (d, $^3J_{HH}$ = 6.9 Hz, 2H, Ph), 7.74 (m, 2H, Ph + C*H*$_{Im\text{-}4,5}$), 7.65 (t, $^3J_{HH}$ = 8.0 Hz, 2H, Ph), 7.51 (t, $^3J_{HH}$ = 8.0 Hz, 2H, Ph), 7.41–7.24 (m overlapped with residual solvent protons, 10H, Ph + Py), 6.85 (d, $^2J_{PH}$ = 3.0 Hz, 1H, C*H*Ph), 3.81–3.71 (m, 1.6H, OC*H*$_2$CH$_2$), 1.91–1.82 (m, 1.6H, OCH$_2$C*H*$_2$). $^{31}$P{$^1$H} NMR (162.0 MHz, $CDCl_3$, 25 °C): δ –6.5 (s). $^{13}$C{$^1$H} NMR (100.6 MHz, $CDCl_3$, 25 °C): δ 149.1 (s, *C*H$_{Py}$), 145.6 (s, *C*$_{ipso\ Py}$), 140.7 (s, *C*H$_{Im\text{-}2}$), 134.3 (d, $^1J_{CP}$ = 14.5 Hz, *C*$_{ipso\ PPh2}$), 134.0 (d, $J_{CP}$ = 21.9 Hz, *C*H$_{PPh2}$), 133.6 (d, $J_{CP}$ = 20.3 Hz, *C*H$_{PPh2}$), 133.2 (br s, *C*H$_{Ph}$), 133.0 (d, $^1J_{CP}$ = 14.2 Hz, *C*$_{ipso\ PPh2}$), 131.5 (d, $^2J_{CP}$ = 8.9 Hz, *C*$_{ipso\ Ph}$), 130.2 (s, *C*H$_{Py}$), 130.0 (s, *C*H$_{Ph}$), 129.7 (s, *C*H$_{PPh2}$), 129.6 (d, $J_{CP}$ = 10.1 Hz, *C*H$_{PPh2}$), 129.4 (d, $J_{CP}$ = 8.3 Hz, *C*H$_{PPh2}$), 129.0 (d, $J_{CP}$ = 8.0 Hz, *C*H$_{Ph}$), 125.4 (s, *C*H$_{Py}$), 120.9 (d, $^3J_{CP}$ = 7.0 Hz, *C*H$_{Im\text{-}4,5}$), 119.5 (s, *C*H$_{Im\text{-}4,5}$), 114.0 (s, *C*H$_{Py}$), 68.1 (s, O*C*H$_2$CH$_{2\ THF}$), 64.2 (d, $^1J_{CP}$ = 14.8 Hz, P*C*(H)Ph), 25.7 (s, O*C*H$_2$CH$_{2\ THF}$). Anal. Calcd. for $C_{27}H_{23}BF_4N_3P$×0.4THF (M = 536.3) C, 64.07; H, 4.93; N, 7.84. Found: C, 63.77; H, 4.63; N, 7.74.

**Generation of free carbene 3 for NMR characterization.** A 0.5M solution of KHMDS in toluene (110 μL, 0.055 mmol) was added dropwise to a suspension of [**3**·H]$BF_4$×0.4THF (27 mg, 0.05 mmol) in toluene (2 mL) at r.t. leading to an orange solution of the corresponding free NHC **3**. The reaction mixture was sonicated for 5 min, stirred for additional 5 min and evaporated under vacuum. The orange residue was dissolved in dry $C_6D_6$ and filtered through Celite directly to the NMR tube. The stability of **3** under these conditions was evaluated by the comparison of the integral intensity of the C*H*Ph signal at 6.06 ppm to the methyl group of residual toluene solvent at 2.11 ppm used as internal standard (*t* = 0 h, 1:2.51, 100% of **3**; *t* = 24 h, 1:3.13, 80% of **3**; *t* = 48 h, 1:4.07, 61.5% of **3**).

**3**: $^1$H NMR (400.1 MHz, $C_6D_6$, 25 °C): δ 8.55 (d, $^3J_{HH}$ = 8.3 Hz, 1H, Py), 8.17 (br s, 1H, C*H*$_{Im\text{-}4,5}$), 8.11 (d, $^3J_{HH}$ = 4.0 Hz, 1H, Py), 7.57 (t, $^3J_{HH}$ = 6.9 Hz, 2H, Ph), 7.31–7.21 (m, 4H, Ph), 7.07–7.04 (m, 1H, Ph), 6.99–6.83 (m, 10H, Ph + Py + C*H*$_{Im\text{-}4,5}$), 6.46 (dd, $^3J_{HH}$ = 7.3 Hz, $^3J_{HH}$ = 5.0 Hz, 1H, Py), 6.06 (d, $^2J_{PH}$ = 5.2 Hz, 1H, C*H*Ph). $^{31}$P{$^1$H} NMR (162.0 MHz, $C_6D_6$, 25 °C): δ –5.7 (s). $^{13}$C{$^1$H} NMR (100.6 MHz, $C_6D_6$, 25 °C): δ 217.0 (d, $^3J_{CP}$ = 25.0

Hz, *C*N$_2$), 154.1 (s, *C*$_{ipso\ Py}$), 147.7 (s, *C*H$_{Py}$), 139.6 (d, $^2J_{CP}$ = 8.9 Hz, *C*$_{ipso\ Ph}$), 137.9 (d, $^1J_{CP}$ = 17.1 Hz, *C*$_{ipso\ PPh2}$), 137.9 (s, *C*H$_{Py}$), 137.7 (d, $^1J_{CP}$ = 15.3 Hz, *C*$_{ipso\ PPh2}$), 135.1 (d, $J_{CP}$ = 20.5 Hz, *C*H$_{PPh2}$), 133.2 (d, $J_{CP}$ = 18.0 Hz, *C*H$_{PPh2}$), 129.1 (s, *C*H$_{Ph}$), 128.9 (d, $J_{CP}$ = 6.6 Hz, *C*H$_{Ph}$), 128.55 (d, $J_{CP}$ = 16.7 Hz, *C*H$_{PPh2}$), 128.5 (br s, *C*H$_{PPh2}$), 121.0 (s, *C*H$_{Py}$), 120.0 (d, $^3J_{CP}$ = 4.2 Hz, *C*H$_{Im-4,5}$), 117.6 (s, *C*H$_{Im-4,5}$), 114.6 (s, *C*H$_{Py}$), 66.6 (d, $^1J_{CP}$ = 9.9 Hz, P*C*(H)Ph).

**Synthesis of complex [4]BF$_4$.** Solid [(cod)RhCl]$_2$ (24.5 mg, 0.05 mmol) was added in one portion to a solution of [**3**·H]BF$_4$×0.4THF (54 mg, 0.1 mmol) in THF (2 mL). After *ca.* 5-10 min of stirring at r.t. [**4**]BF$_4$ started to precipitate as a yellow powder. The resulting suspension was stirred for 2 h and hexane (2 mL) was added dropwise to complete the precipitation. The supernatant was removed by mean cannula tipped with filter paper and the precipitate was washed with hexane (2 mL) and dried under vacuum to give [**4**]BF$_4$ (68 mg, 90%) as yellow powder. Though the dissolution of this complex in common solvents ($CH_2Cl_2$, acetone, MeCN) gradually leads to the formation of Rh$^I$ pincer-type complex **5** and its decomposition products, we were able to fully characterize it by NMR spectroscopy and to grow single crystals suitable for X-ray diffraction experiment by diffusion of ether vapors to a solution of the complex in dichloromethane.

[**4**]BF$_4$: $^1$H NMR (400.1 MHz, $(CD_3)_2CO$, 25 °C): δ 10.06 (s, 1H, C*H*$_{Im-2}$), 8.62–8.52 (m, 3H, Py + Ph), 8.27 (s, 1H, C*H*$_{Im-4,5}$), 8.16 (td overlapped with other m signal, $^3J_{HH}$ = 8.0 Hz, $J_{HH}$ = 1.8 Hz, 1H, Py), 8.14–8.07 (m, 2H, Ph), 7.92 (d, $^3J_{HH}$ = 8.3 Hz, 1H, Py), 7.82 (s, 1H, C*H*$_{Im-4,5}$), 7.73–7.59 (m, 5H, Ph + Py), 7.55–7.45 (m, 3H, Ph), 7.36 (td, $^3J_{HH}$ = 7.9 Hz, $J_{PH}$ = 2.3 Hz, 2H, Ph), 7.26 (d, $^2J_{PH}$ = 8.7 Hz, 1H, C*H*Ph), 7.20 (t, $^3J_{HH}$ = 8.6 Hz, 2H, Ph), 5.80–5.68 (m, 1H, C*H* $_{COD}$), 5.68–5.57 (m, 1H, C*H* $_{COD}$), 3.08–2.95 (m, 2H, C*H* $_{COD}$), 2.64–2.52 (m, 1H, C*H*$_2$ $_{COD}$), 2.51–2.42 (m overlapped with another m, 1H, C*H*$_2$ $_{COD}$), 2.42–2.33 (m overlapped with another m and signal of free COD, 2H, C*H*$_2$ $_{COD}$), 2.28–2.10 (m, 2H, C*H*$_2$ $_{COD}$), 2.02–1.90 (m, 2H, C*H*$_2$ $_{COD}$). $^{31}$P{$^1$H} NMR (162.0 MHz, $(CD_3)_2CO$, 25 °C): δ 36.5 (d, $^1J_{RhP}$ = 157.3 Hz). $^{13}$C{$^1$H} NMR (100.6 MHz, $(CD_3)_2CO$, 25 °C): δ 150.3 (s, *C*H$_{Py}$), 147.2 (s, *C*$_{ipso\ Py}$), 141.3 (s, *C*H$_{Py}$), 137.4 (br d, $^1J_{CP}$ = 12.7 Hz, *C*$_{ipso\ PPh2}$), 136.8 (br s, *C*H$_{Im-2}$), 134.4 (s, *C*$_{ipso\ Ph}$), 134.1 (d, $J_{CP}$ = 9.7 Hz, *C*H$_{PPh2}$), 133.2 (s, *C*H$_{Ph}$), 132.1 (br s, *C*H$_{Ph}$), 131.4 (s, *C*H$_{Ph}$), 130.6 (s, *C*H$_{PPh2}$), 129.7 (d, $J_{CP}$ = 10.0 Hz, *C*H$_{PPh2}$), 129.4 (d, $J_{CP}$ = 9.1 Hz, *C*H$_{PPh2}$), 126.4 (s, *C*H$_{Py}$), 125.2 (br s, *C*H$_{Im-4,5}$), 119.6 (s, *C*H$_{Im-4,5}$), 115.2 (s, *C*H$_{Py}$), 108.1 (br s, *C*H $_{COD}$), 74.2–73.6 (br m, *C*H $_{COD}$), 65.1 (d, $^1J_{CP}$ = 14.8 Hz, P*C*(H)Ph), 33.4 (br s, *C*H$_2$ $_{COD}$), 33.2 (br s, *C*H$_2$ $_{COD}$), 29.6 (br s overlapped with residual solvent signal, *C*H$_2$ $_{COD}$). Anal. Calcd. for $C_{35}H_{35}BClF_4N_3PRh$ (M = 753.8) C, 55.77; H, 4.68; N, 5.57. Found: C, 55.47; H, 4.65; N, 5.37.

**Generation of complex 5 for NMR characterization.** A solution of KHMDS in THF-*d*$_8$ (10 mg in *ca.* 0.2 mL of deuterated solvent) was added dropwise to a yellow suspension of [**4**]BF$_4$ (37.5 mg, 0.05 mmol) in THF-*d*$_8$ (0.8 mL) at –80°C. The cooling bath was removed causing the reaction mixture to turn orange, then red-orange, and some of the target product precipitated. The solution was filtered through Celite directly to the NMR tube and rapidly

analyzed by $^{1}H$ and $^{31}P\{^{1}H\}$ to confirm the formation of **5** as major organometallic product together with free 1,5-cyclooctadiene (integration intensities for some aromatic could not be correctly determined due to the superposition with impurities). The low solubility and/or gradual decomposition of **5** precluded further characterization by $^{13}C\{^{1}H\}$ NMR regardless the solvent we considered ($CD_2Cl_2$, acetone-$d_6$, $CD_3CN$).

**5**: $^{1}H$ NMR (400.1 MHz, THF-$d_8$, 25 °C): δ 9.38 (br s, 1H, Py), 8.20 (dd, $J_{PH}$ = 9.4 Hz, $^{3}J_{HH}$ = 9.4 Hz, 2H, Ph), 8.03 (t, $^{3}J_{HH}$ = 7.5 Hz, 1H, Py), 7.69–7.62 (m, 3H, Ph + C*H*$_{Im\text{-}4,5}$), 7.59 (d, $^{3}J_{HH}$ = 8.2 Hz, 1H, Py), 7.46–6.97 (m, 7H integration intensity is overestimated due to the superposition with impurities, Ph + Py), 6.78 (d, $^{3}J_{HH}$ = 2.2 Hz, 1H, C*H*$_{Im\text{-}4,5}$), 6.01 (d, $^{2}J_{PH}$ = 5.7 Hz, 1H, C*H*Ph). $^{31}P\{^{1}H\}$ NMR (162.0 MHz, THF-$d_8$, 25 °C): δ 84.3 (d, $^{1}J_{RhP}$ = 234.0 Hz).

**Synthesis of complex 7.** Solid $[Rh(cod)Cl]_2$ (42 mg, 0.085 mmol) was added to a solution of [**3**·H]$BF_4$×0.4THF (91 mg, 0.17 mmol) in THF (10 mL) at r.t. and the reaction mixture was stirred for 1 h, time after which $^{31}P\{^{1}H\}$ NMR monitoring revealed the complete transformation of [**3**·H]$BF_4$ into [**4**]$BF_4$ (δ 35.3 (d, $^{1}J_{RhP}$ = 157.0 Hz)). The yellow reaction mixture was cooled to –80°C and a 0.5M solution of KHMDS in toluene (340 μL, 0.17 mmol) was then added in a dropwise fashion. After 5 min the cooling bath was removed causing the reaction mixture to turn orange, then red-orange, while reaching r.t.. At this stage, $^{31}P\{^{1}H\}$ NMR monitoring indicates the formation of complex **5** (δ 86.7 (d, $^{1}J_{RhP}$ = 234.0 Hz)). The solution was cooled to –80°C again, and solid iodine (43 mg, 0.17 mmol) was added in one portion. After stirring for 10 min at –80°C, the cooling bath was removed allowing the red-brown reaction mixture to reach r.t.. $^{31}P\{^{1}H\}$ NMR (δ 69.9 (d, $^{1}J_{RhP}$ = 128.9 Hz)) and ESI mass spectroscopy (m/z 684.17 ($M^+$–I), 776.08 ($M^+$–Cl)) analyses of an aliquot of the reaction mixture gave evidences for the exclusive formation of **6**. An excess of solid KI (282 mg, 1.7 mmol) and few drops of water were added at r.t. to the reaction, which was stirred at room temperature overnight. The volatiles were removed under vacuum and the red-brown residue was purified by column chromatography on silica (6×3 cm). Deep red band of the product was eluted with THF/toluene 1:2 mixture, giving after the evaporation of the solvents under vacuum complex **7** (126 mg, 74%) as red microcrystalline solid. Single crystals of **7** suitable for X-ray diffraction experiments were obtained by slow concentration of its solution in THF/toluene mixture at room temperature.

**7**: $^{1}H$ NMR (400.1 MHz, THF-$d_8$, 25 °C): δ 9.75 (br t, $^{3}J_{HH}$ = 4.8 Hz, $^{4}J_{PH}$ = 4.8 Hz, 1H, Py), 8.21 (dd, $J_{PH}$ = 11.6 Hz, $^{3}J_{HH}$ = 7.8 Hz, 2H, Ph), 8.17 (d, $^{3}J_{HH}$ = 2.1 Hz, 1H, C*H*$_{Im\text{-}4,5}$), 8.13 (t, $^{3}J_{HH}$ = 7.9 Hz, 1H, Py), 7.88 (d, $^{3}J_{HH}$ = 8.2 Hz, 1H, Py), 7.84 (br d, $^{3}J_{HH}$ = 6.3 Hz, 2H, Ph), 7.78 (dd, $J_{PH}$ = 11.5 Hz, $^{3}J_{HH}$ = 7.9 Hz, 2H, Ph), 7.52 (t, $^{3}J_{HH}$ = 6.4 Hz, 1H, Py), 7.39–7.21 (m, 8H, Ph + C*H*$_{Im\text{-}4,5}$ + C*H*Ph), 7.05 (t, $^{3}J_{HH}$ = 7.4 Hz, 1H, Ph), 6.94–6.86 (m, 2H, Ph). $^{1}H$ NMR (400.1 MHz, dmso-$d_6$, 25 °C): δ 9.49 (br t, $^{3}J_{HH}$ = 4.9 Hz, $^{4}J_{PH}$ = 4.9 Hz, 1H, Py), 8.63 (d, $^{3}J_{HH}$ = 2.4 Hz, 1H, C*H*$_{Im\text{-}4,5}$), 8.38–8.28 (m, 2H, Py + Ph), 8.14–8.06 (m, 2H, Ph), 7.84–7.70 (m, 3H, Ph + Py), 7.68–7.59 (m, 3H, Ph + Py), 7.53 (d, $^{3}J_{HH}$ = 2.4 Hz, 1H, C*H*$_{Im\text{-}$

$_{4,5}$), 7.44–7.29 (m, 6H, Ph), 7.19–7.13 (m, 1H, Ph), 7.05 (td, $^3J_{HH}$ = 2.0 Hz, $J_{PH}$ = 0.5 Hz, 2H, Ph). $^{31}P\{^1H\}$ NMR (162.0 MHz, THF-$d_8$, 25 °C): δ 76.9 (d, $^1J_{RhP}$ = 127.0 Hz). $^{31}P\{^1H\}$ NMR (162.0 MHz, THF-$d_8$, 25 °C): δ 74.4 (d, $^1J_{RhP}$ = 123.5 Hz). $^{13}C\{^1H\}$ NMR (100.6 MHz, dmso-$d_6$, 25 °C): δ 181.7 (dd, $^1J_{RhC}$ = 33.0 Hz, $^2J_{CP}$ = 9.7 Hz, Rh–*C*N$_2$), 152.9 (d, $^3J_{CP}$ = 2.6 Hz, *C*$_{ipso\ Py}$), 152.8 (s, *C*H$_{Py}$), 142.0 (s, *C*H$_{Py}$), 138.0 (d, $^1J_{CP}$ = 54.6 Hz, *C*$_{ipso\ PPh2}$), 136.7 (d, $J_{CP}$ = 9.8 Hz, *C*H$_{PPh2}$), 134.1 (d, $^1J_{CP}$ = 4.8 Hz, *C*$_{ipso\ PPh2}$), 132.4 (d, $J_{CP}$ = 8.8 Hz, *C*H$_{PPh2}$), 130.8 (s, *C*$_{ipso\ Ph}$), 132.5 (d, $J_{CP}$ = 16.9 Hz, *C*H$_{Ph}$), 132.4 (d, $J_{CP}$ = 20.3 Hz, *C*H$_{Ph}$), 129.8 (s, *C*H$_{Py}$), 129.1 (s, *C*H$_{PPh2}$), 128.0 (d, $J_{CP}$ = 11.3 Hz, *C*H$_{PPh2}$), 126.7 (d, $J_{CP}$ = 11.0 Hz, *C*H$_{PPh2}$), 124.0 (d, $J_{CP}$ = 3.7 Hz, *C*H$_{Ph}$), 123.2 (d, $^3J_{CP}$ = 9.4 Hz, *C*H$_{Im-4,5}$), 119.8 (s, *C*H$_{Im-4,5}$), 113.4 (s, *C*H$_{Py}$), 67.8 (d, $^1J_{CP}$ = 37.2 Hz, P*C*(H)Ph). Anal. Calcd. for $C_{27}H_{22}I_3N_3PRh\times C_6H_5CH_3$ (M = 995.2) C, 41.03; H, 3.04; N, 4.22. Found: C, 41.56; H, 2.91; N, 4.13.

**Synthesis of complex 8**. Solid $[NiBr_2(NC$*i*$-Pr)]_n$ (40.3 mg, 0.14 mmol) and $NEt_3$ (22 μL, 0.155 mmol) were added consecutively to a yellow solution of [**3**·H]$BF_4\times$0.4THF (75 mg, 0.14 mmol) in MeCN (1.0 mL). The resulting emerald green reaction mixture was heated to 60 °C for 2 h, leading to a yellow solution with precipitation of deep red crystals of **8**, some of them been suitable for X-ray diffraction analysis. The reaction mixture was allowed to cool to r.t. and the precipitate was filtered off, washed with MeCN (2×1 mL), ether (2×1 mL), and dried under vacuum to give the main portion of complex **8** (47 mg). The combined filtrate and acetonitrile washings were evaporated under vacuum at 50 °C to *ca.* a half of original volume and left to stand overnight at room temperature leading to a crystallization of additional amount of **8**. The second crop of the product (13 mg) was obtained as described above to afford the desired complex **8** (60 mg, 67% of combined yield) as red-brown powder.

**8**: $^1H$ NMR (500.3 MHz, dmso-$d_6$, 25 °C): δ 8.85 (br d, $^3J_{HH}$ = 4.0 Hz, 1H, Py), 8.54 (s, 1H, C*H*$_{Im-4,5}$), 8.48 (t, $^3J_{HH}$ = 6.9 Hz, 1H, Py), 8.20 (br d, $^3J_{HH}$ = 8.5 Hz, 1H, Py), 8.15–8.05 (m, 2H, Ph), 7.75 (d, $^3J_{HH}$ = 7.3 Hz, 2H, Ph), 7.71–7.63 (m, 3H, Ph + C*H*$_{Im-4,5}$), 7.59 (dd, $J_{PH}$ = 11.2 Hz, $^3J_{HH}$ = 7.7 Hz, 2H, Ph), 7.41 (t, $^3J_{HH}$ = 6.4 Hz, 1H, Ph), 7.23 (t, $^3J_{HH}$ = 7.2 Hz, 2H, Ph), 7.17–7.00 (m, 6H, Ph + Py + C*H*Ph). $^{31}P\{^1H\}$ NMR (202.5 MHz, dmso-$d_6$, 25 °C): δ 68.5 (s). $^{13}C\{^1H\}$ NMR (125.8 MHz, dmso-$d_6$, 25 °C): δ 170.5 (d, $^2J_{CP}$ = 49.8 Hz, Ni–*C*N$_2$), 151.1 (s, *C*$_{ipso\ Py}$), 150.1 (s, *C*H$_{Py}$), 143.8 (s, *C*H$_{Py}$), 135.3 (d, $J_{CP}$ = 10.3 Hz, *C*H$_{PPh2}$), 133.1 (d, $J_{CP}$ = 9.3 Hz, *C*H$_{PPh2}$), 132.8 (s, *C*$_{ipso\ Ph}$), 132.4 (br d, $J_{CP}$ = 3.0 Hz, *C*H$_{Ph}$), 129.4 (d, $J_{CP}$ = 10.8 Hz, *C*H$_{PPh2}$), 128.9 (s, *C*H$_{Py}$), 128.5 (s, *C*H$_{PPh2}$), 128.1 (d, $J_{CP}$ = 11.2 Hz, *C*H$_{PPh2}$), 127.4 (s, *C*H$_{Ph}$), 125.6 (d, $^1J_{CP}$ = 46.5 Hz, *C*$_{ipso\ PPh2}$), 124.3 (s, *C*H$_{Ph}$), 124.2 (d, $^1J_{CP}$ = 48.2 Hz, *C*$_{ipso\ PPh2}$), 122.9 (d, $^3J_{CP}$ = 9.2 Hz, *C*H$_{Im-4,5}$), 121.0 (s, *C*H$_{Im-4,5}$), 111.9 (s, *C*H$_{Py}$), 70.3 (d, $^1J_{CP}$ = 41.2 Hz, P*C*(H)Ph). Anal. Calcd. for $C_{27}H_{22}N_3PNiBr_2$: C, 50.83; H, 3.48; N, 6.59; Found: C, 50.48; H, 3.56; N, 6.77.

**X-ray Diffraction Studies.** Data were collected on a Bruker D8/APEX II/Incoatec IμS Microsource diffractometer ([**4**]$BF_4$ and **7**) or a Bruker D8/APEX II/molten gallium anode diffractometer (**8**). All calculations were performed on a PC compatible computer using the WinGX system.[S6] Full crystallographic data are given in Table S1. The structures were solved using the SIR92 program,[S7] which revealed in each instance the position of most of the non-hydrogen atoms. All the remaining non-hydrogen atoms were located by the usual combination of full matrix least-squares refinement and difference electron density syntheses using the SHELX program.[S8] Atomic scattering factors were taken from the usual tabulations. Anomalous dispersion terms for the Rh, Ni, I, Br, Cl, and/or P atoms were included in Fc. All non-hydrogen atoms were allowed to vibrate anisotropically. The hydrogen atoms were generally set in idealized positions ($R_3CH$, C–H = 0.96 Å; $R_2CH_2$, C–H = 0.97 Å; $RCH_3$, C–H = 0.98 Å; $C(sp^2)$–H = 0.93 Å; $U_{iso}$ 1.2 or 1.5 times greater than the $U_{eq}$ of the carbon atom to which the hydrogen atom is attached) and their positions refined as "riding" atoms expect for H41, H44, H45, and H48 in the structure of [**4**]$BF_4$, whose position were inferred from a residual electron density map and refined with a $U_{iso}$ arbitrarily set at 0.035 $Å^2$. CCDC 1556215-1556217 contain the supplementary crystallographic data for the three structures unveiled in this paper. These data can be obtained free of charge from the Cambridge Crystallographic Data Centre via www.ccdc.cam.ac.uk/data_request/cif.

**Table S1.** Crystal data and structures refinements for complexes [**4**]$BF_4$, **7**, and **8**

| Complex | [**4**]$BF_4$ | **7**.toluene | **8** |
|---|---|---|---|
| empirical formula | $C_{35}H_{35}ClN_3PRh,BF_4$ | $C_{27}H_{22}I_3N_3PRh,C_7H_8$ | $C_{27}H_{22}Br_2N_3NiP$ |
| $M_r$ | 753.80 | 995.19 | 637.97 |
| $T$/ K | 100 | 100 | 100 |
| λ /Å | 0.71073 | 0.71073 | 1.34139 |
| Crystal system | triclinic | monoclinic | monoclinic |
| Space group (no.) | P-1 (#2) | P21/c (# 14) | P21/c (# 14) |
| $a$/ Å | 9.2988(2) | 12.9780(3) | 13.7320(11) |
| $b$/ Å | 14.5983(3) | 15.1277(3 | 7.9816(6) |
| $c$/ Å | 13.2821(3) | 17.3050(4) | 23.4948(18) |
| $\alpha$/ ° | 81.853(1) | | |
| $\beta$/ ° | 73.402(1) | 92.288(1) | 96.728(3) |
| $\gamma$/ ° | 72.649(1) | | |
| $V$/ Å$^3$ | 1646.10(6) | 3394.74(13) | 2557.4(3) |
| $Z$ | 2 | 4 | 4 |
| $D_c$/ g.cm$^{-3}$ | 1.521 | 1.947 | 1.657 |
| μ/ mm$^{-1}$ | 0.702 | 3.06 | 7.064 |
| F(000) | 768 | 1896 | 1272 |
| $\theta_{max}$/ ° | 26.4 | 26.4 | 26.4 |
| Completeness to $\theta_{max}$ (%) | 0.99 | 0.99 | 0.99 |
| Index range, *hkl* | -11<h<11<br>-16<k<16<br>-18<l<18 | -11<h<11<br>-16<k<16<br>-18<l<18 | -17<h<17<br>-10<k<10<br>-30<l<25 |
| Reflections collected | 96636 | 119877 | 42082 |
| Independent reflections | 6735 | 6940 | 5881 |
| Parameters | 427 | 380 | 307 |
| *GOF* | 1.08 | 1.11 | 1.07 |
| $R$ [I>2σ(I)] | 0.0189 | 0.0223 | 0.0289 |
| $R_w$ [I>2σ(I)] | 0.0469 | 0.0258 | 0.0299 |
| $R$ (all data) | 0.0219 | 0.0560 | 0.0776 |
| Rw (all data) | 0.0487 | 0.0525 | 0.0769 |
| $\Delta\rho_{max/min}$/ e.Å$^{-3}$ | -0.34/0.99 | -0.91, 1.30 | -0.34/1.06 |

**Table S2**. Selected bond distances (Å) and angles (°) for complex [**4**]$BF_4$

**Bond Distances**

| | | |
|---|---|---|
| Rh1 | -Cl1 | 2.3755(4) |
| Rh1 | -P1 | 2.2868(5) |
| Rh1 | -C41 | 2.2166(17) |
| Rh1 | -C44 | 2.1366(17) |
| Rh1 | -C45 | 2.1140(16) |
| Rh1 | -C48 | 2.2404(19) |
| P1 | -C4 | 1.8975(15) |
| P1 | -C21 | 1.8195(16) |
| P1 | -C31 | 1.8389(15) |
| N1 | -C1 | 1.3325(19) |
| N1 | -C2 | 1.388(2) |
| N1 | -C5 | 1.436(2) |
| N2 | -C1 | 1.325(2) |
| N2 | -C3 | 1.387(2) |
| N2 | -C4 | 1.4841(19) |
| N3 | -C9 | 1.342(2) |
| C2 | -C3 | 1.348(2) |
| C4 | -C11 | 1.514(2) |

**Bond Angles**

| | | | |
|---|---|---|---|
| Cl1 | -Rh1 | -P1 | 91.00(2) |
| Rh1 | -P1 | -C4 | 118.78(5) |
| Rh1 | -P1 | -C21 | 112.26(5) |
| Rh1 | -P1 | -C31 | 118.50(5) |
| C4 | -P1 | -C21 | 102.03(7) |
| C4 | -P1 | -C31 | 100.70(7) |
| C21 | -P1 | -C31 | 102.02(7) |
| C1 | -N1 | -C2 | 108.56(13) |
| C1 | -N1 | -C5 | 123.64(14) |
| C2 | -N1 | -C5 | 127.65(13) |
| C1 | -N2 | -C3 | 108.31(13) |
| C1 | -N2 | -C4 | 125.96(13) |
| C3 | -N2 | -C4 | 125.67(14) |
| N1 | -C1 | -N2 | 108.96(14) |
| N1 | -C2 | -C3 | 106.65(14) |
| N2 | -C3 | -C2 | 107.51(15) |
| P1 | -C4 | -N2 | 111.72(9) |
| P1 | -C4 | -C11 | 111.75(10) |
| N2 | -C4 | -C11 | 111.80(13) |
| N1 | -C5 | -N3 | 113.80(13) |
| N1 | -C5 | -C6 | 120.40(15) |
| N3 | -C5 | -C6 | 125.80(16) |

**Table S3**. Selected bond distances (Å) and angles (°) for complex **7**

**Bond Distances**

| | | |
|---|---|---|
| I1 | -Rh1 | 2.6729(4) |
| I2 | -Rh1 | 2.7450(5) |
| I3 | -Rh1 | 2.6756(4) |
| Rh1 | -P1 | 2.2769(8) |
| Rh1 | -N3 | 2.176(3) |
| Rh1 | -C1 | 1.894(3) |
| P1 | -C4 | 1.939(3) |
| P1 | -C21 | 1.823(3) |
| P1 | -C31 | 1.814(3) |
| N1 | -C1 | 1.351(4) |
| N1 | -C2 | 1.403(4) |
| N1 | -C5 | 1.402(4) |
| N2 | -C1 | 1.326(4) |
| N2 | -C3 | 1.403(4) |
| N2 | -C4 | 1.462(4) |
| C2 | -C3 | 1.342(4) |
| C4 | -C11 | 1.508(5) |

**Bond Angles**

| | | | |
|---|---|---|---|
| I1 | -Rh1 | -I2 | 92.48(1) |
| I1 | -Rh1 | -I3 | 169.64(2) |
| I1 | -Rh1 | -P1 | 93.21(2) |
| I1 | -Rh1 | -N3 | 84.95(7) |
| I1 | -Rh1 | -C1 | 89.22(8) |
| I2 | -Rh1 | -I3 | 91.26(1) |
| I2 | -Rh1 | -P1 | 103.95(2) |
| I2 | -Rh1 | -N3 | 98.80(7) |
| I2 | -Rh1 | -C1 | 174.88(9) |
| I3 | -Rh1 | -P1 | 95.27(2) |
| I3 | -Rh1 | -N3 | 84.93(7) |
| I3 | -Rh1 | -C1 | 86.27(9) |
| P1 | -Rh1 | -N3 | 157.24(7) |
| P1 | -Rh1 | -C1 | 80.77(9) |
| N3 | -Rh1 | -C1 | 76.53(11 |
| Rh1 | -P1 | -C4 | 103.22(9) |
| C1 | -N1 | -C2 | 108.8(2) |
| C1 | -N1 | -C5 | 116.5(3) |
| C2 | -N1 | -C5 | 134.7(3) |
| C1 | -N2 | -C3 | 109.3(2) |
| C1 | -N2 | -C4 | 120.1(2) |
| C3 | -N2 | -C4 | 130.6(3) |
| N1 | -C5 | -N3 | 113.0(3) |
| Rh1 | -N3 | -C9 | 129.1(2) |
| C5 | -N3 | -C9 | 118.0(3) |
| Rh1 | -C1 | -N1 | 120.9(2) |
| Rh1 | -C1 | -N2 | 131.2(2) |
| N1 | -C1 | -N2 | 107.9(3) |
| N1 | -C2 | -C3 | 106.8(3) |
| N2 | -C3 | -C2 | 107.3(3) |
| 1 | -C4 | -N2 | 104.69(19) |
| P1 | -C4 | -C11 | 116.5(2) |

**Table S4**. Selected bond distances (Å) and angles (°) for complex **8**

**Bond Distances**

| | | |
|---|---|---|
| Br1 | -Ni1 | 2.3542(4) |
| Br2 | -Ni1 | 2.6845(5) |
| Ni1 | -P1 | 2.1534(6) |
| Ni1 | -N3 | 2.0334(17) |
| Ni1 | -C1 | 1.797(2) |
| P1 | -C4 | 1.9008(18) |
| P1 | -C21 | 1.812(2) |
| P1 | -C31 | 1.802(2) |
| N1 | -C1 | 1.356(3) |
| N1 | -C2 | 1.404(3) |
| N1 | -C5 | 1.409(3) |
| N2 | -C1 | 1.339(3) |
| N2 | -C3 | 1.394(3) |
| N2 | -C4 | 1.473(3) |
| N3 | -C5 | 1.350(3) |
| C2 | -C3 | 1.352(3) |
| C4 | -C11 | 1.509(3) |
| C5 | -C6 | 1.382(3) |

**Bond Angles**

| | | | |
|---|---|---|---|
| Br1 | -Ni1 | -Br2 | 98.14(1) |
| Br1 | -Ni1 | -P1 | 95.06(2) |
| Br1 | -Ni1 | -N3 | 99.33(5) |
| Br1 | -Ni1 | -C1 | 164.24(7) |
| Br2 | -Ni1 | -P1 | 110.97(2) |
| Br2 | -Ni1 | -N3 | 92.77(5) |
| Br2 | -Ni1 | -C1 | 97.61(6) |
| P1 | -Ni1 | -N3 | 150.15(5) |
| P1 | -Ni1 | -C1 | 79.49(7) |
| N3 | -Ni1 | -C1 | 79.64(8) |
| Ni1 | -P1 | -C4 | 105.91(6) |
| Ni1 | -P1 | -C21 | 109.21(7) |
| Ni1 | -P1 | -C31 | 124.95(8) |
| C4 | -P1 | -C21 | 104.44(10) |
| C4 | -P1 | -C31 | 104.11(9) |
| C21 | -P1 | -C31 | 106.42(9) |
| C1 | -N1 | -C2 | 109.71(17) |
| C1 | -N1 | -C5 | 114.83(17) |
| C2 | -N1 | -C5 | 135.01(17) |
| C1 | -N2 | -C3 | 110.34(17) |
| C1 | -N2 | -C4 | 117.14(16) |
| C3 | -N2 | -C4 | 131.97(16) |
| Ni1 | -N3 | -C5 | 114.35(13) |
| Ni1 | -N3 | -C9 | 128.03(14) |
| C5 | -N3 | -C9 | 117.58(17) |
| Ni1 | -C1 | -N1 | 120.26(16) |
| Ni1 | -C1 | -N2 | 133.11(15) |
| N1 | -C1 | -N2 | 106.46(18) |
| N1 | -C2 | -C3 | 106.39(19) |
| N2 | -C3 | -C2 | 107.1(2) |
| P1 | -C4 | -N2 | 100.49(11) |
| P1 | -C4 | -C11 | 115.22(13) |
| N2 | -C4 | -C11 | 113.58(17) |
| N1 | -C5 | -N3 | 110.86(16) |

## References


S1 D. A. Valyaev, O. A. Filippov, N. Lugan, G. Lavigne, N. A. Ustynyuk, *Angew. Chem. Int. Ed.,* 2015, **54**, 6315.

S2 A. Raba, M. R. Anneser, D. Jantke, M. Cokoja, W. A. Herrmann and F. E. Kühn, *Tetrahedron Lett.,* 2013, **54**, 3384.

S3 G. Giordano and R. H. Crabtree, *Inorg. Synth.,* 1990, **28**, 88.

S4 B. Vabre, D. M. Spasyuk and D. Zargarian, *Organometallics,* 2012, **31**, 8561.

S5 G. R. Fulmer, A. J. M. Miller, N. H. Sherden, H. E. Gottlieb, A. Nudelman, B. M. Stoltz, J. E. Bercaw and K. I. Goldberg, *Organometallics,* 2010, **29**, 2176.

S6 L. J. Farrugia, *J. Appl. Crystallogr.*, 1999, **32**, 837.

S7 A. Altomare, G. Cascarano, C. Giacovazzo, A. Guagliardi, *J. Appl. Crystallogr.*, 1994, **27**, 435.

S8 G. M. Sheldrick, *Acta Crystallogr.*, 2008, **A64**, 112.

**Figure S1**. $^{1}$H NMR spectrum of [**2**]$BF_4$ (400.1 MHz, $CDCl_3$, 25°C), signal of residual *N*-(2-pyridyl)imidazole and $CH_2Cl_2$ are marked with asterisk

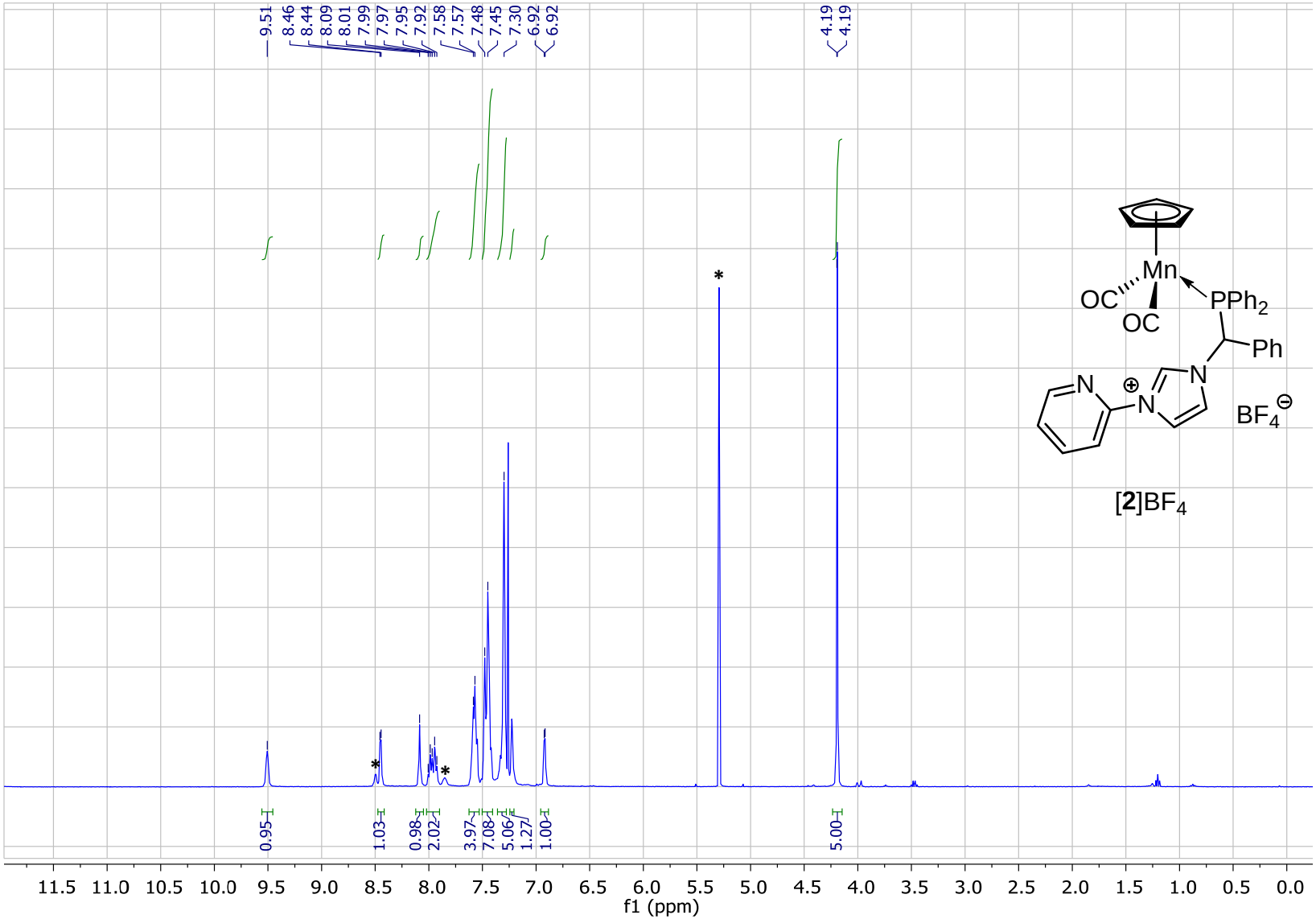

**Figure S2**. $^{31}P\{^{1}H\}$ NMR spectrum of of [**2**]$BF_4$ (162.0 MHz, $CDCl_3$, 25°C)

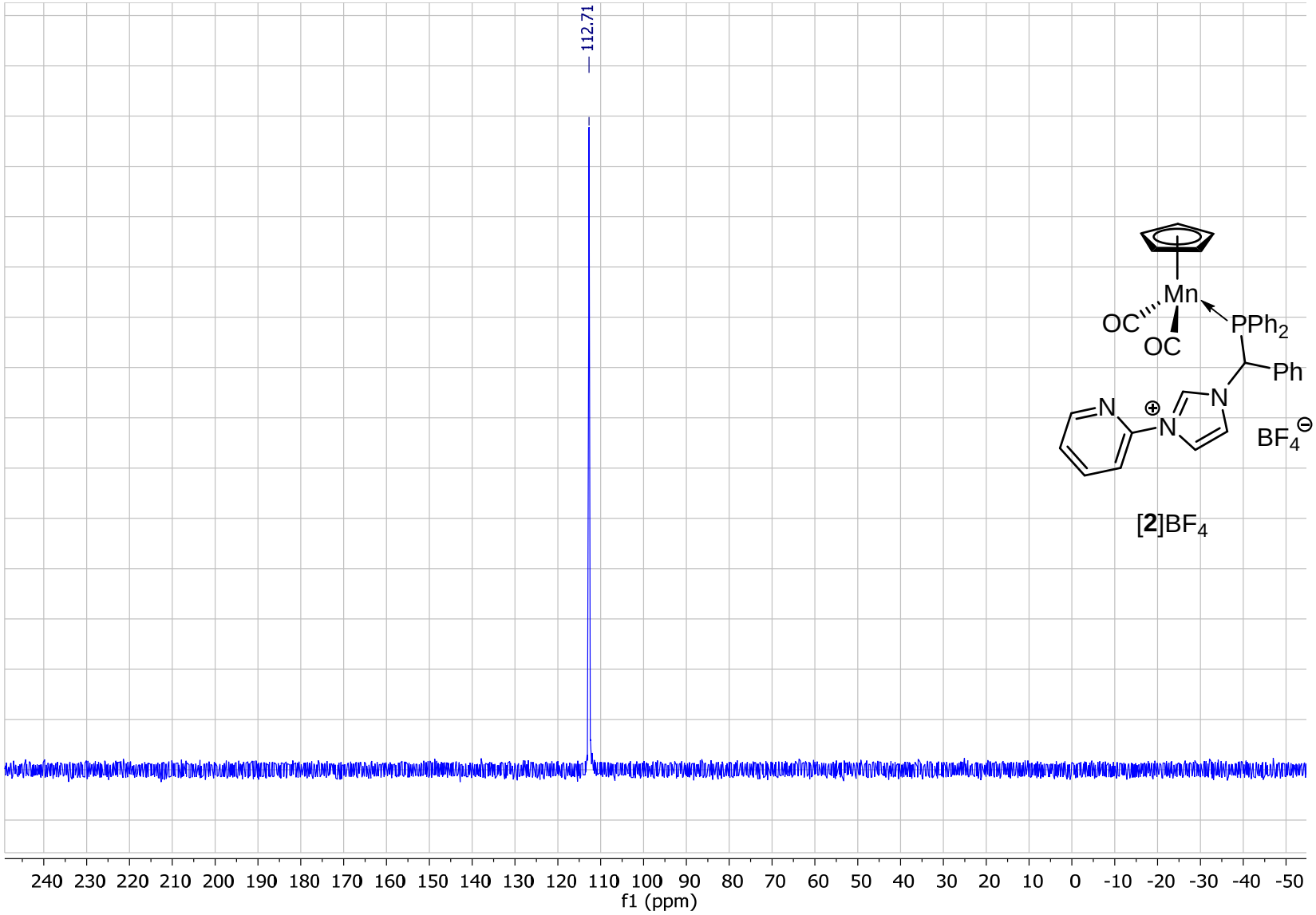

**Figure S3**. $^{1}H$ NMR spectrum of [**3**·H]$BF_4$×0.4THF (400.1 MHz, $CDCl_3$, 25°C)

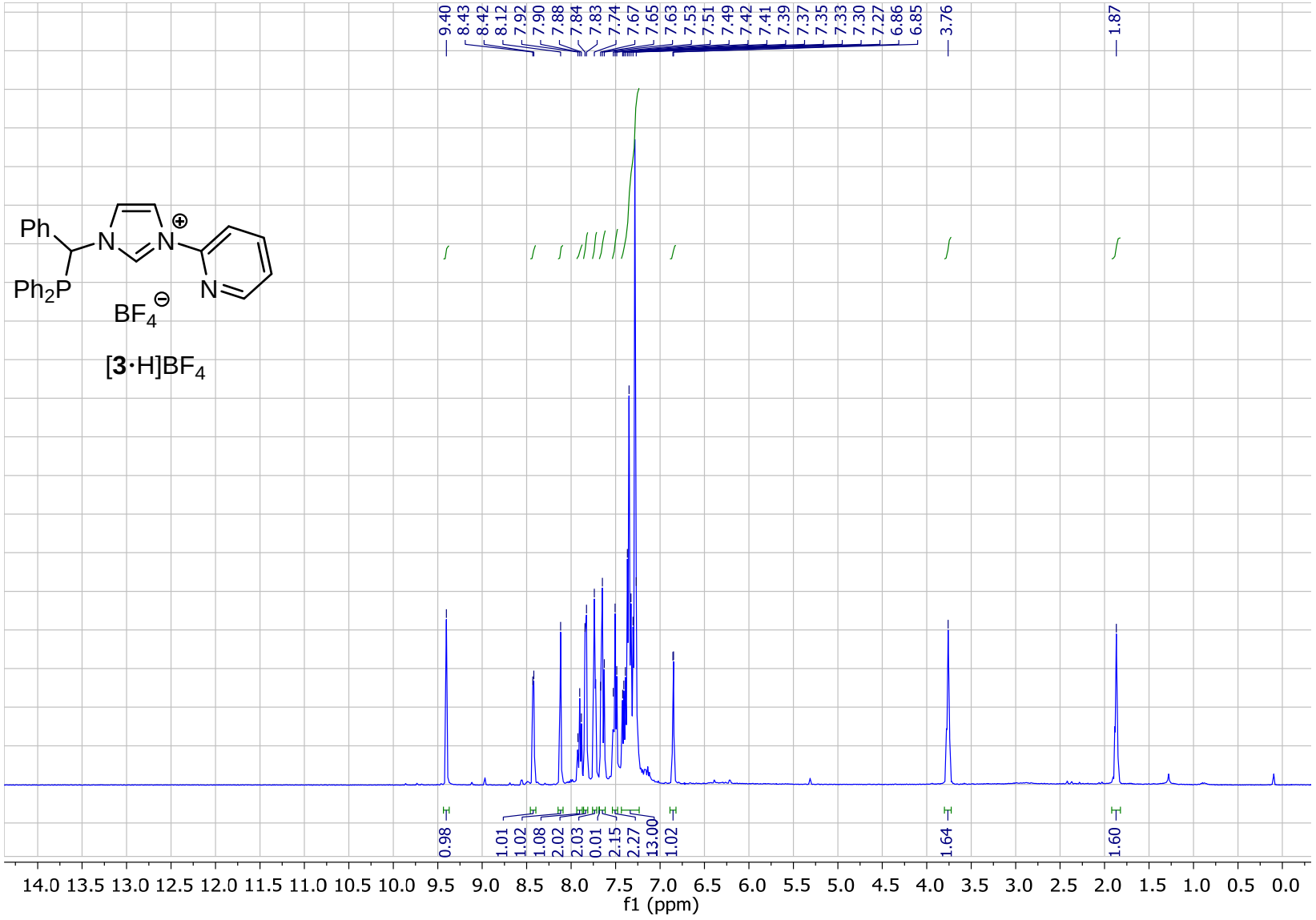

**Figure S4**. $^{31}P\{^{1}H\}$ NMR spectrum of [**3**·H]$BF_4$×0.4THF (162.0 MHz, $CDCl_3$, 25°C)

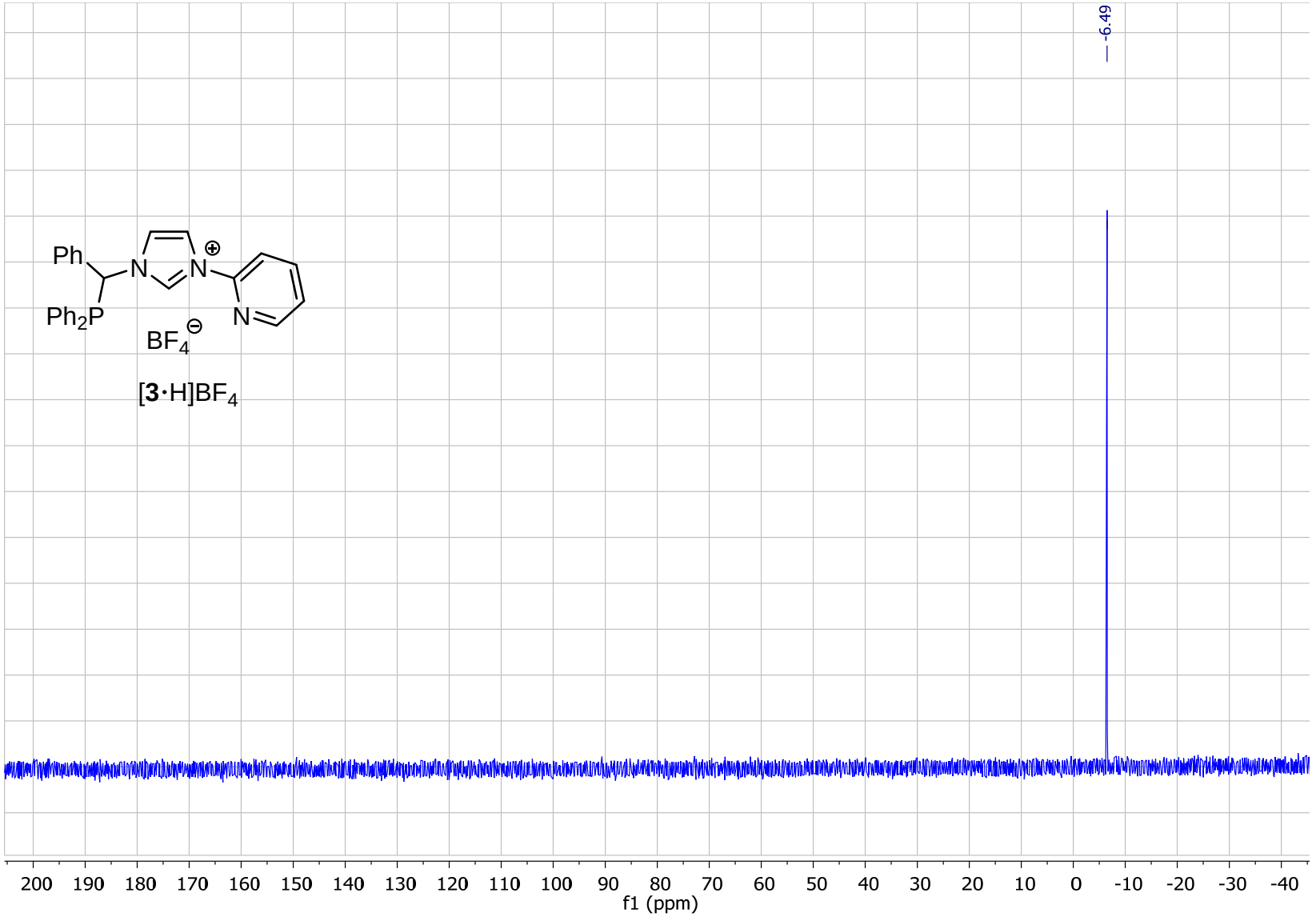

**Figure S5**. $^{13}C\{^{1}H\}$ NMR spectrum of [**3**·H]$BF_4$×0.4THF (100.6 MHz, $CDCl_3$, 25 °C)

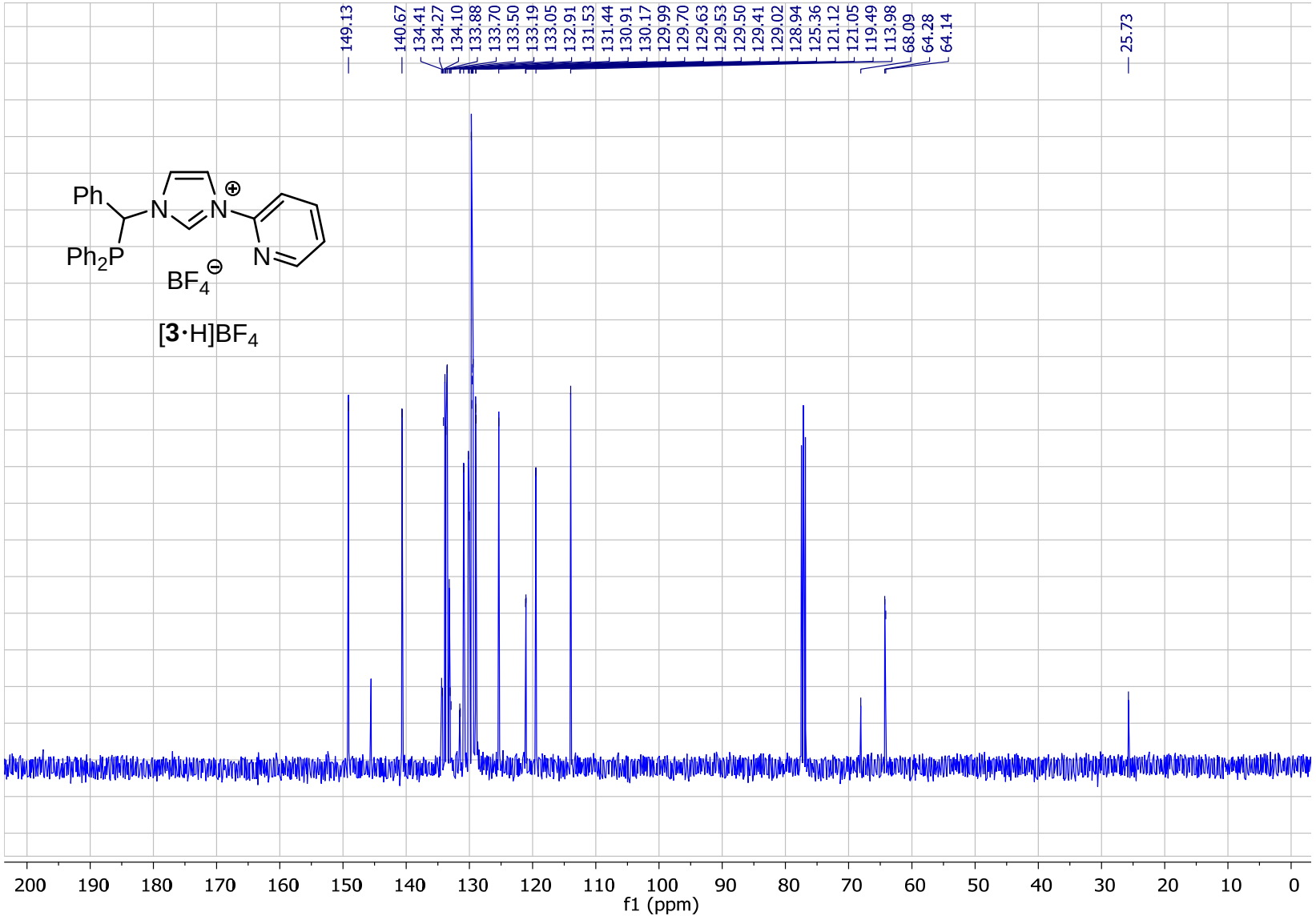

**Figure S6**. $^{13}C\{^{1}H, ^{31}P\}$ NMR spectrum of [**3**·H]$BF_4$×0.4THF (100.6 MHz, $CDCl_3$, 25 °C)

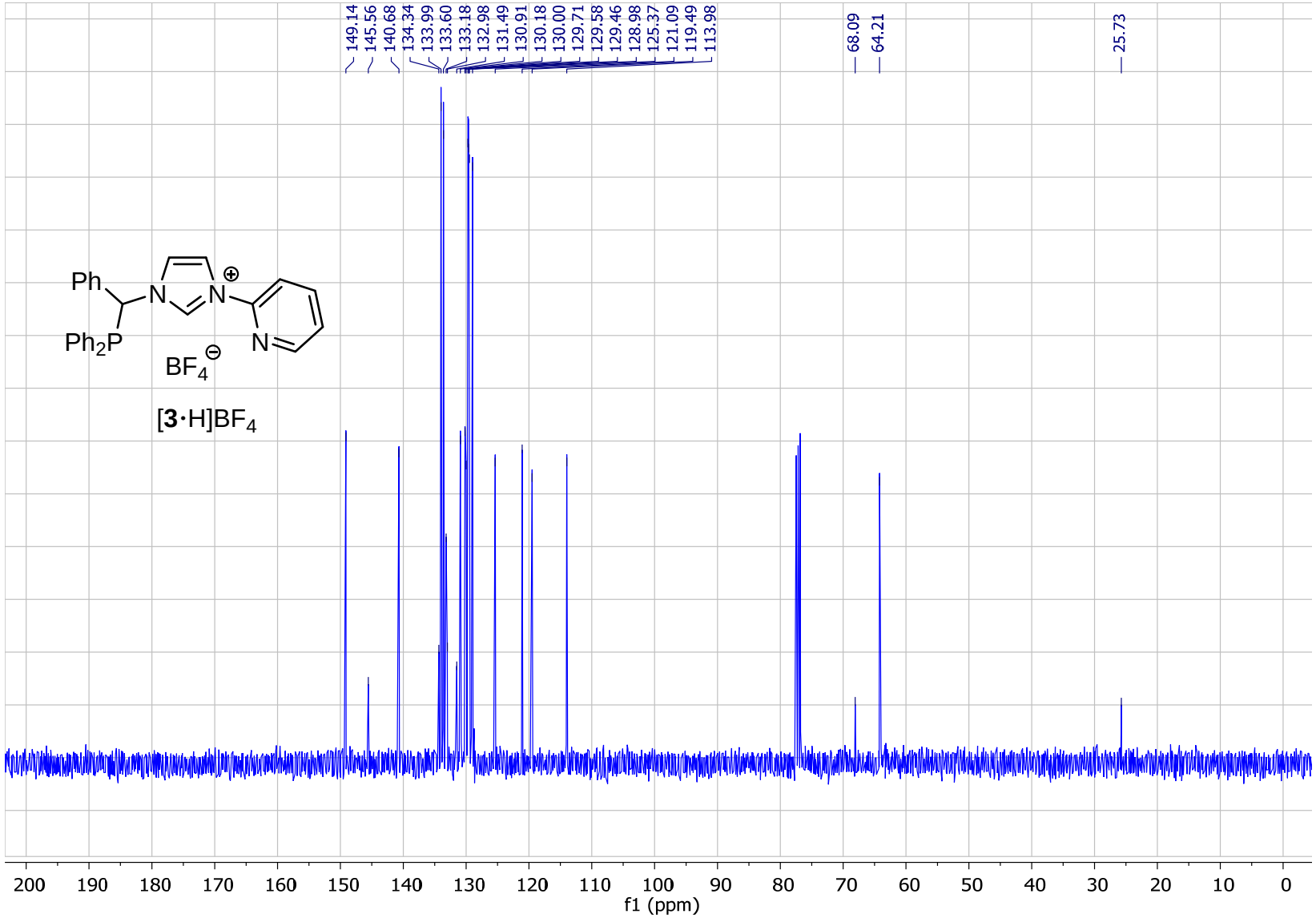

**Figure S7**. $^{1}$H NMR spectrum of **3** (400.1 MHz, $C_6D_6$, 25°C), signals of residual toluene and HMDS are marked with asterisk

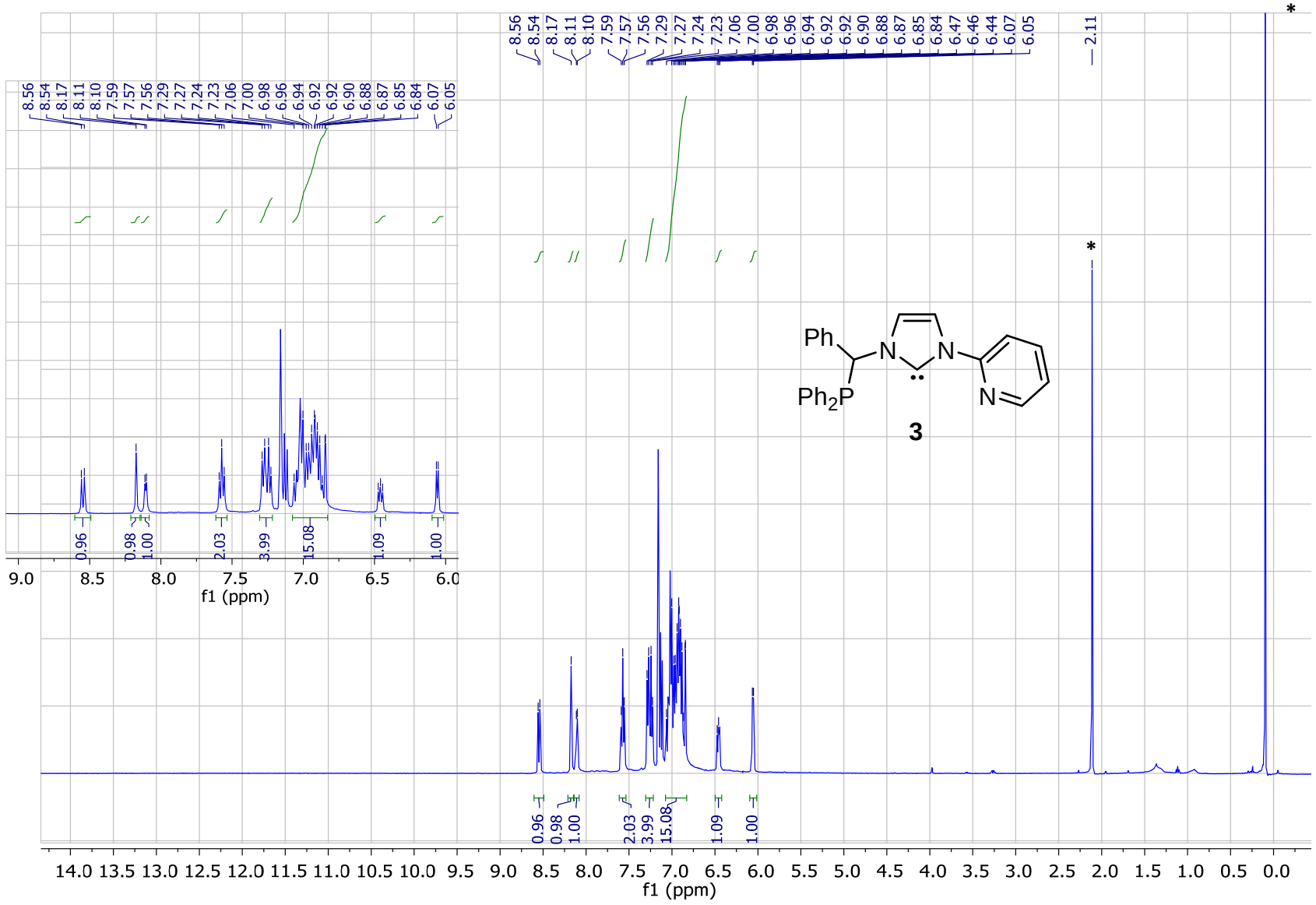

**Figure S8**. $^{31}P\{^{1}H\}$ NMR spectrum of **3** (162.0 MHz, $C_6D_6$, 25 °C)

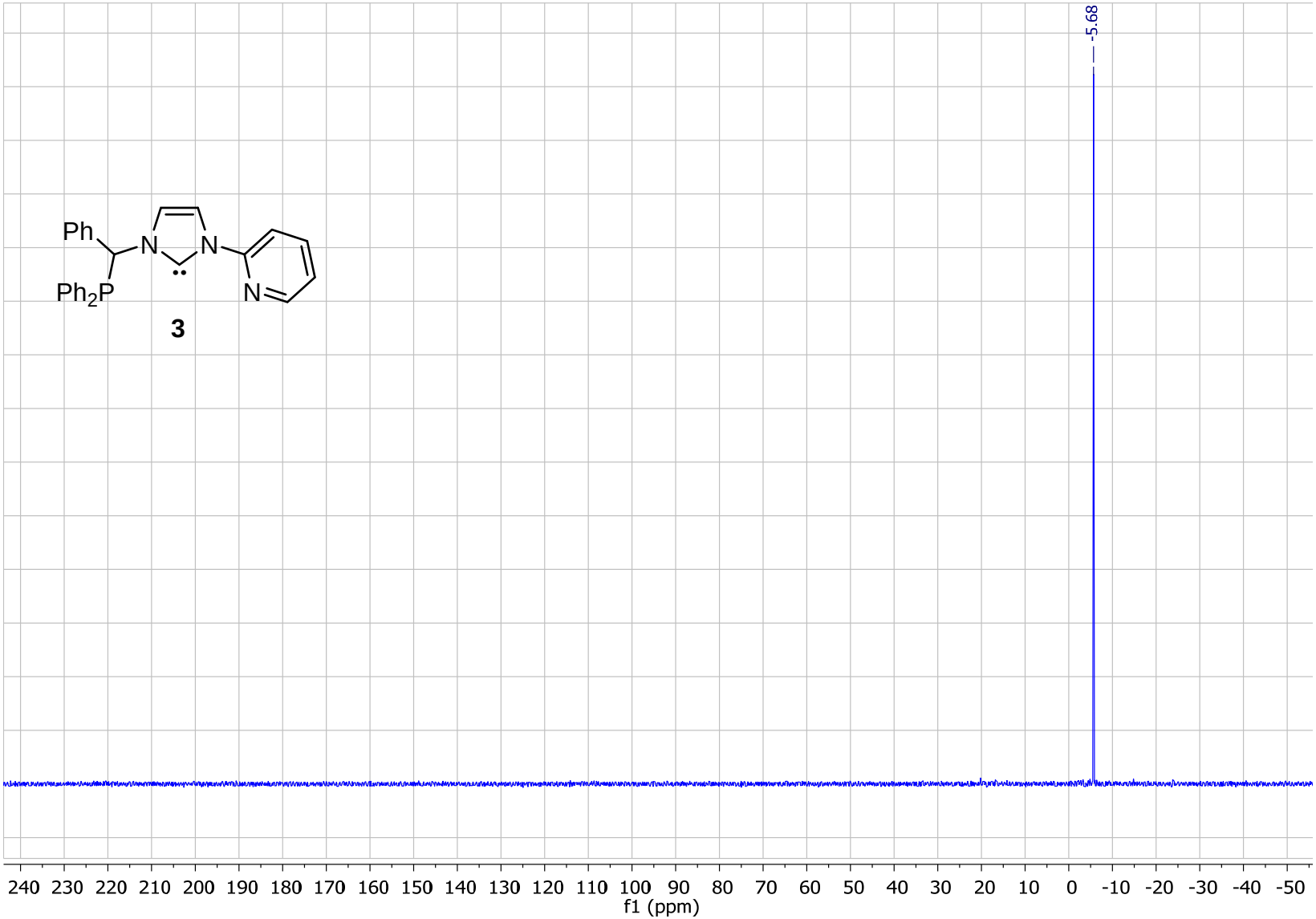

**Figure S9**. $^{13}C\{^{1}H\}$ NMR spectrum of **3** (100.6 MHz, $C_6D_6$, 25°C), signals of residual toluene and HMDS are marked with asterisk

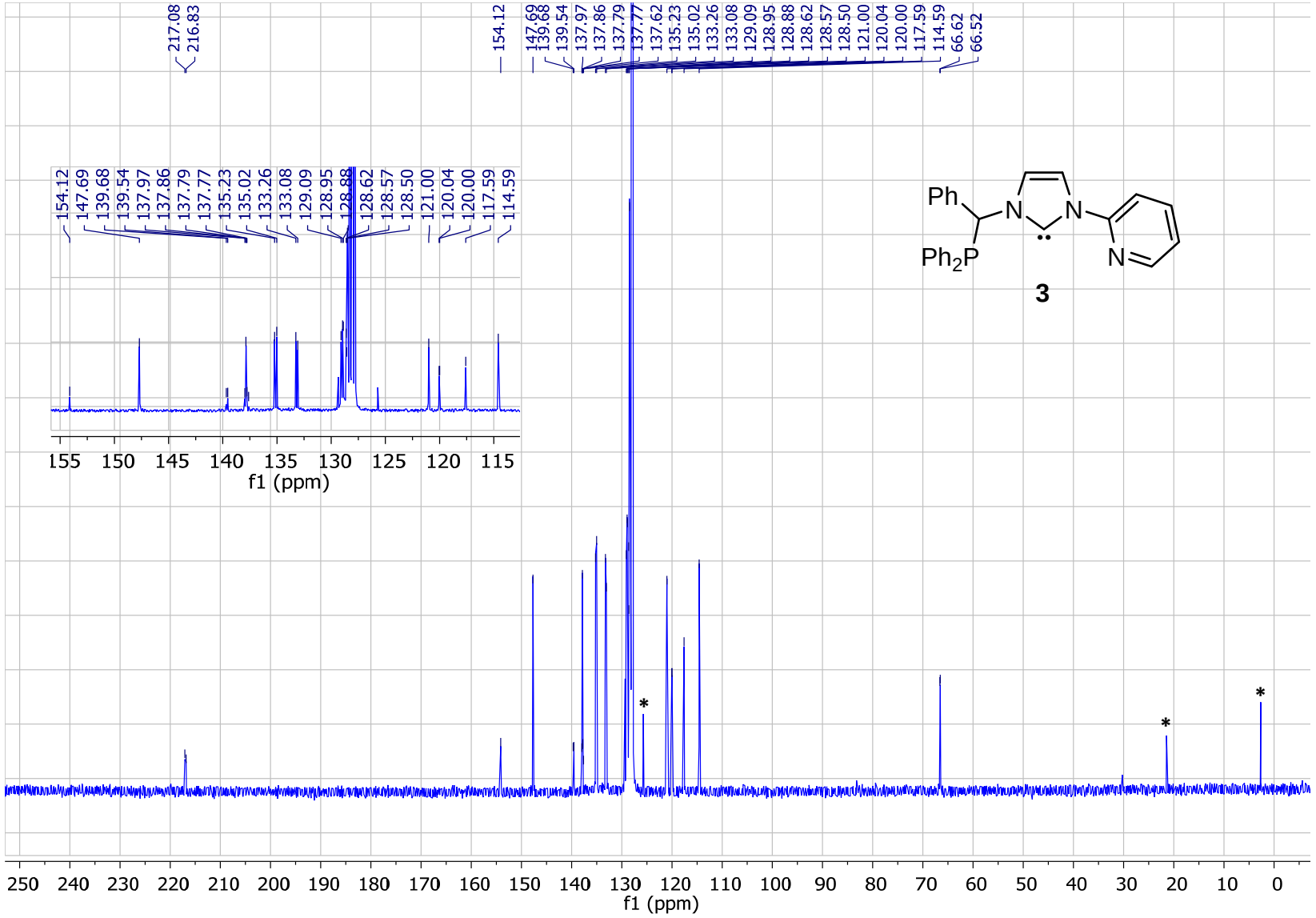

**Figure S10**. $^{1}H$ NMR spectrum of [**4**]$BF_4$ (400.1 MHz, $(CD_3)_2CO$, 25°C), signals of residual water (*), THF (■) and free 1,5-cyclooctadiene (●) are indicated with the corresponding markers

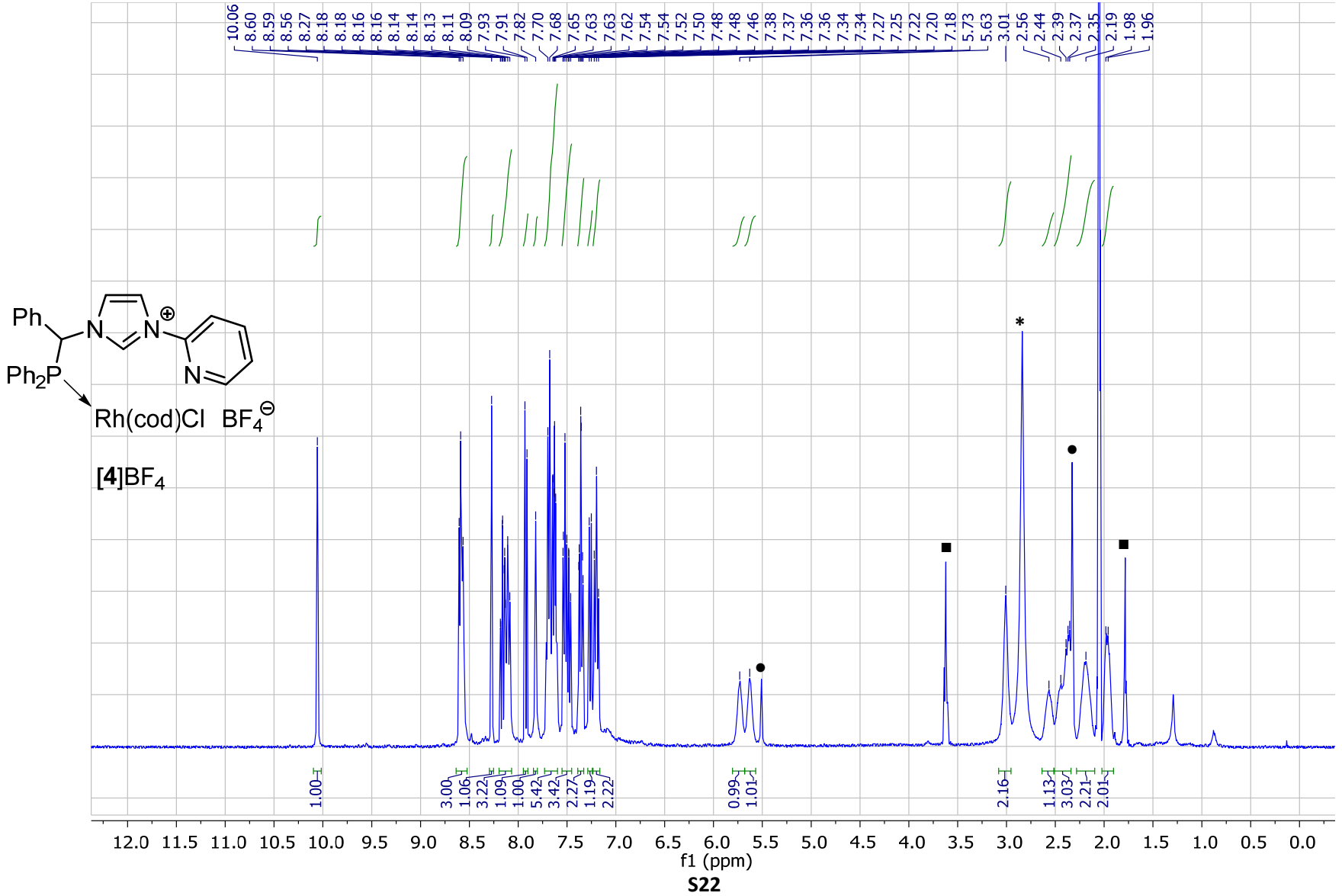

**Figure S11**. Section of $^{1}H$-$^{1}H$ COSY NMR spectrum of [**4**]$BF_4$ (400.1 MHz, $(CD_3)_2CO$, 25°C), signals of residual water (*), THF (■) and free 1,5-cyclooctadiene (●) are indicated with the corresponding markers

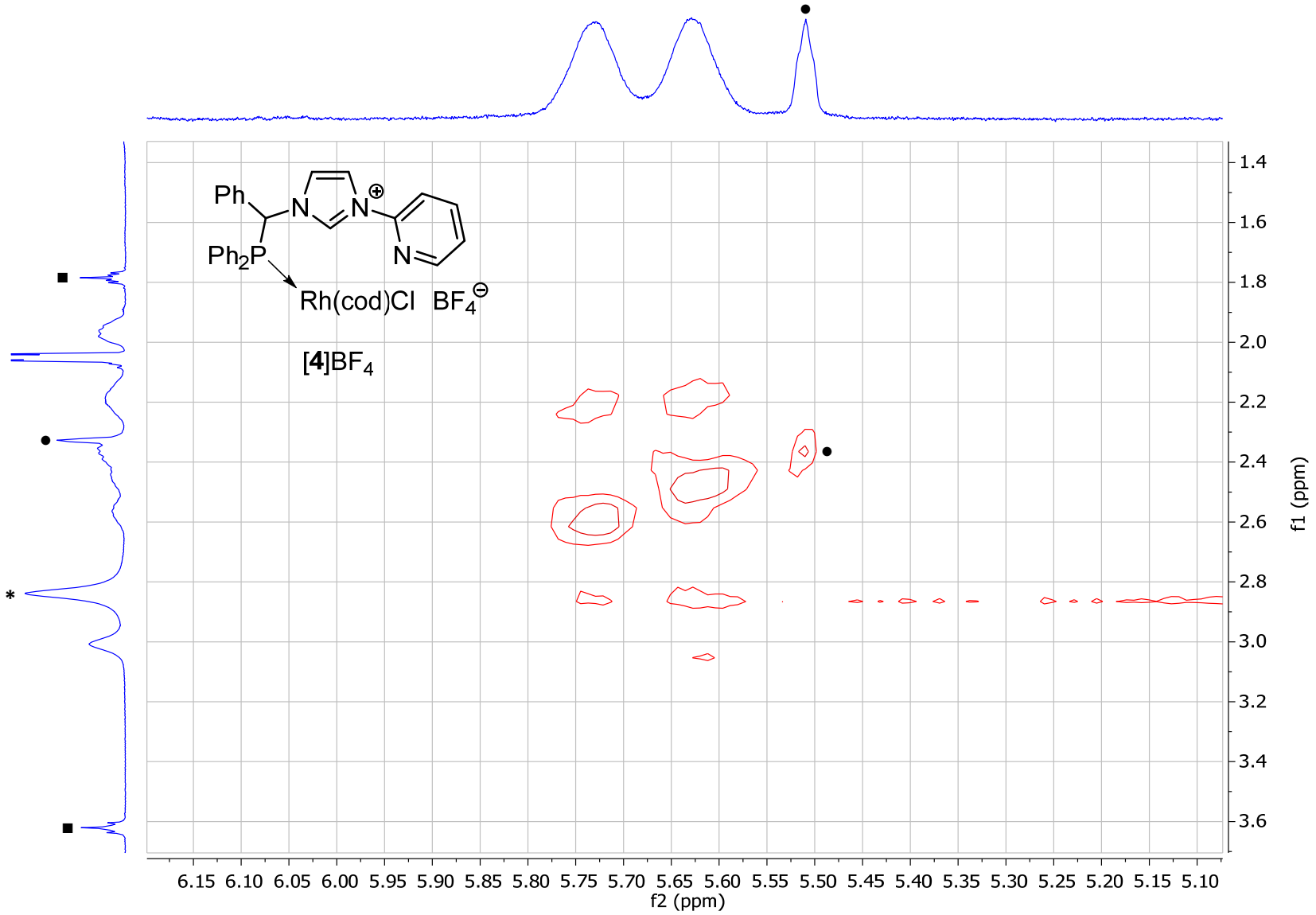

**Figure S12**. $^{31}P\{^{1}H\}$ NMR spectrum of [**4**]$BF_4$ (162.0 MHz, $(CD_3)_2CO$, 25°C)

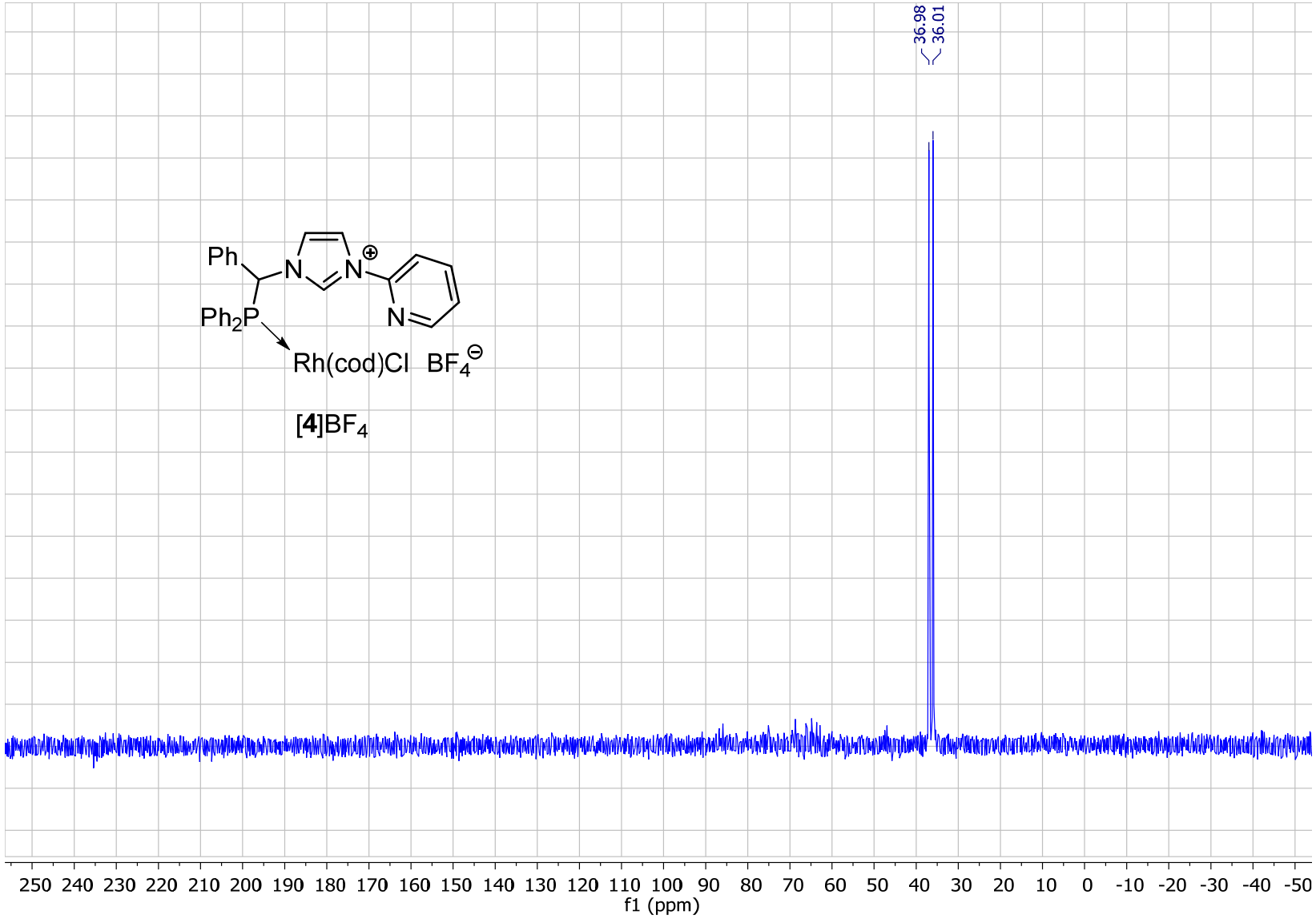

**Figure S13**. $^{13}C\{^{1}H\}$ NMR spectrum of [**4**]$BF_4$ (100.6 MHz, $(CD_3)_2CO$, 25°C)

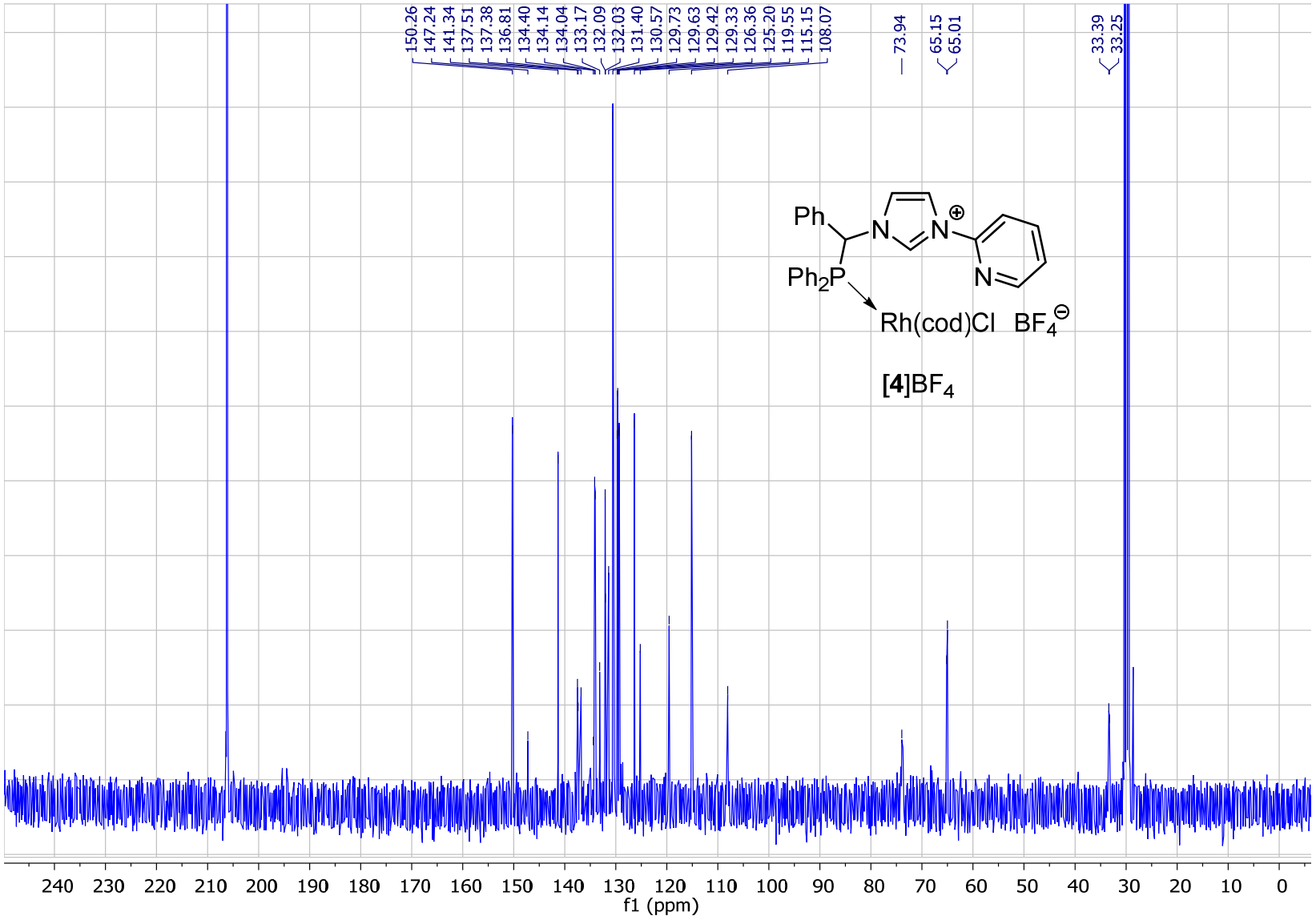

**Figure S14**. $^{13}C\{^{1}H\}$-$^{1}H$ HMQC NMR spectrum of [**4**]$BF_4$ (100.6 MHz, $(CD_3)_2CO$, 25°C)

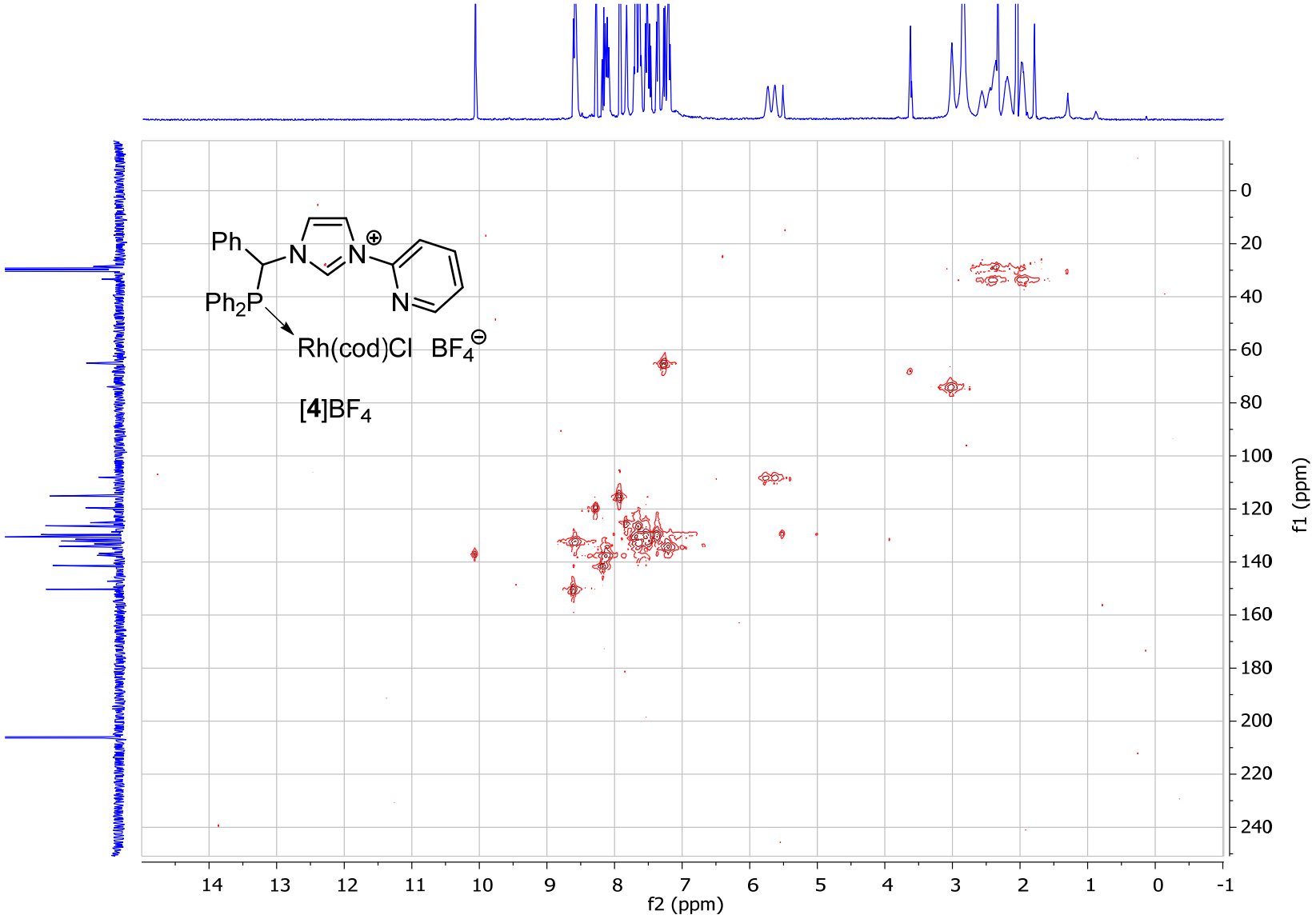

**Figure S15**. $^{1}$H NMR spectru m of **5** (400.1 MHz, THF-$d_8$, 25°C), signals of residual HMDS (*) and free 1,5-cyclooctadiene (●) are indicated with the corresponding markers

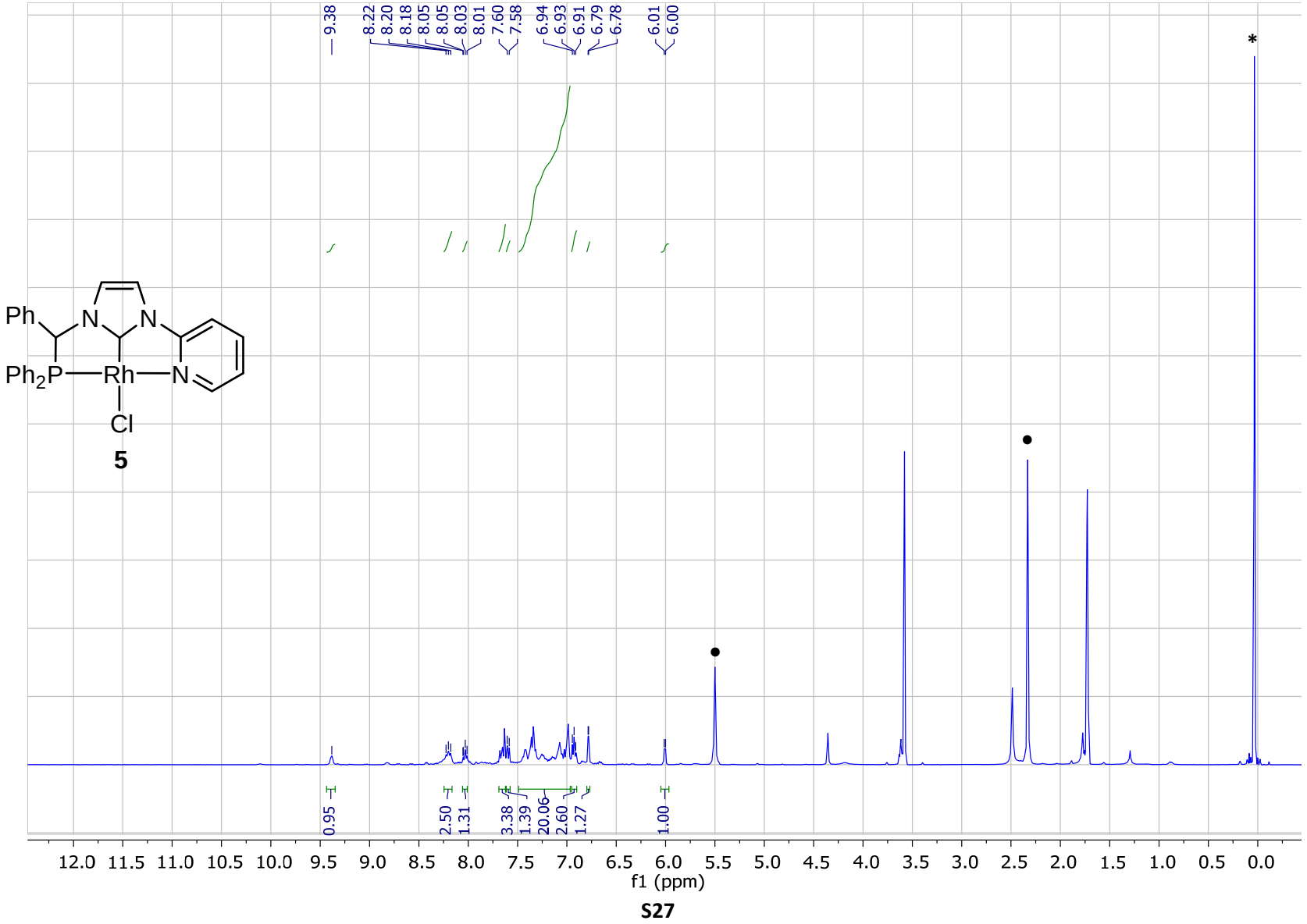

**Figure S16**. $^{31}P\{^{1}H\}$ NMR spectrum of **5** (162.0 MHz, THF-$d_8$, 25°C)

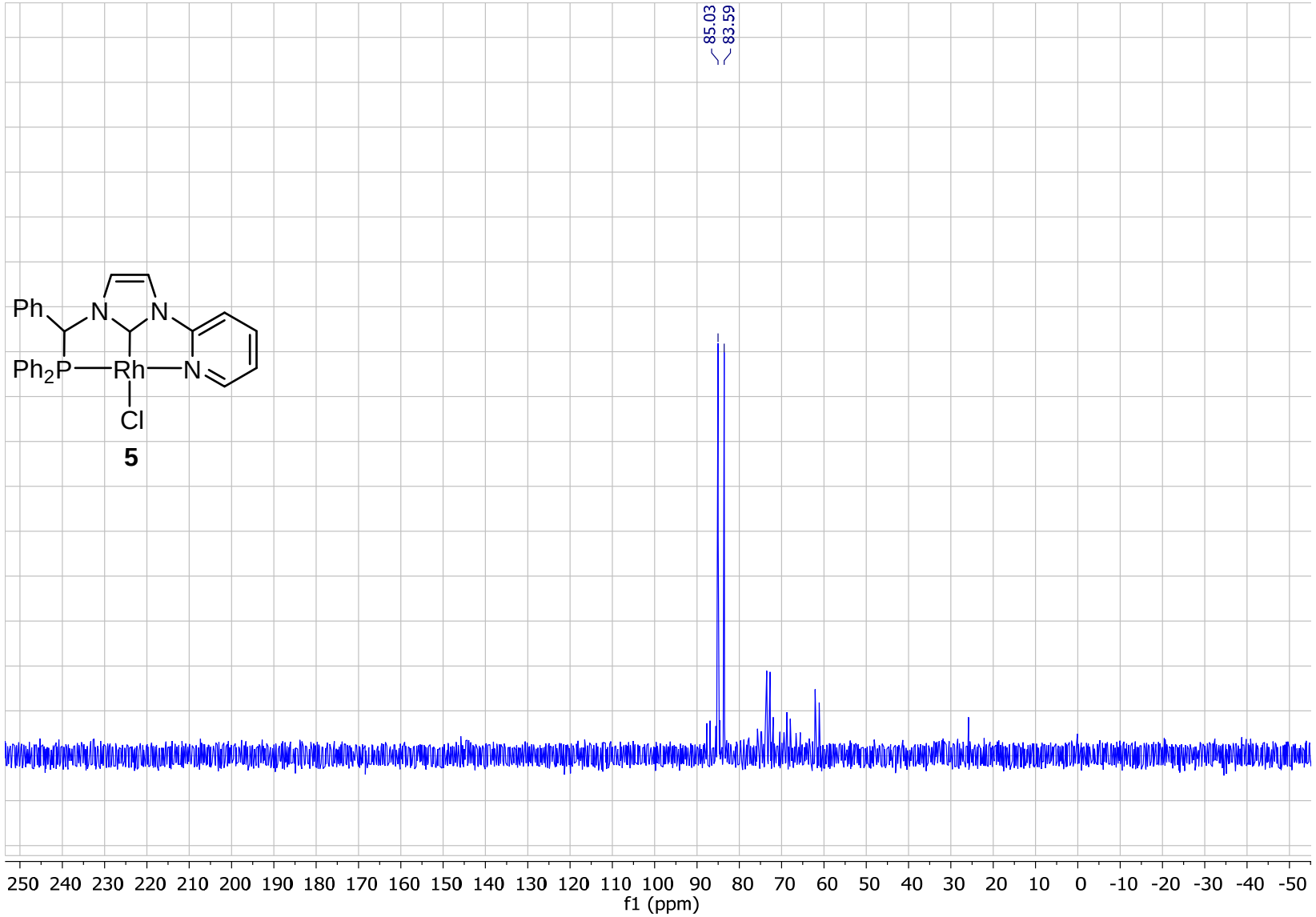

**Figure S17**. $^{31}P\{^{1}H\}$ NMR monitoring of transformation [**3**·H]$BF_4$ → [**4**]$BF_4$ → **5** → **6** → **7** (162.0 MHz, diluted THF solution with $C_6D_6$ capillary, 25°C)

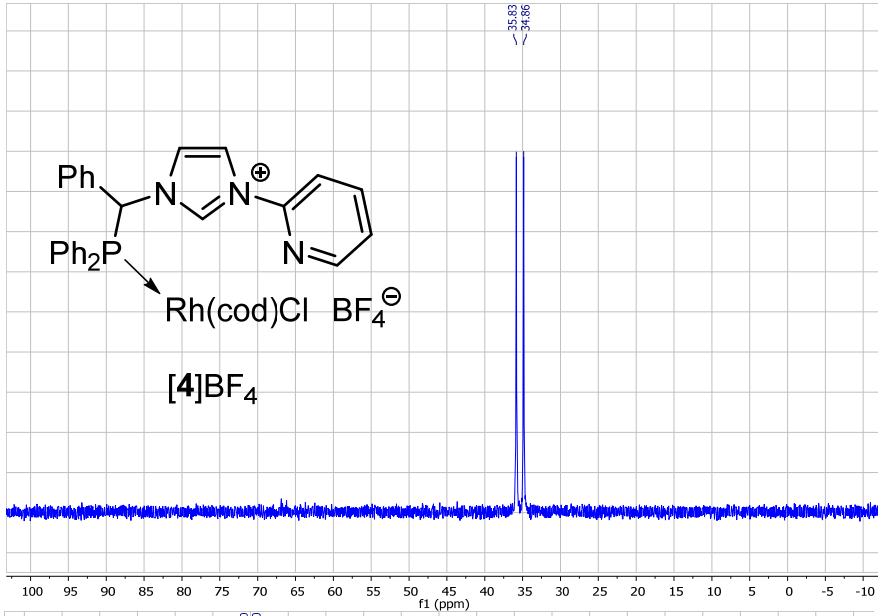


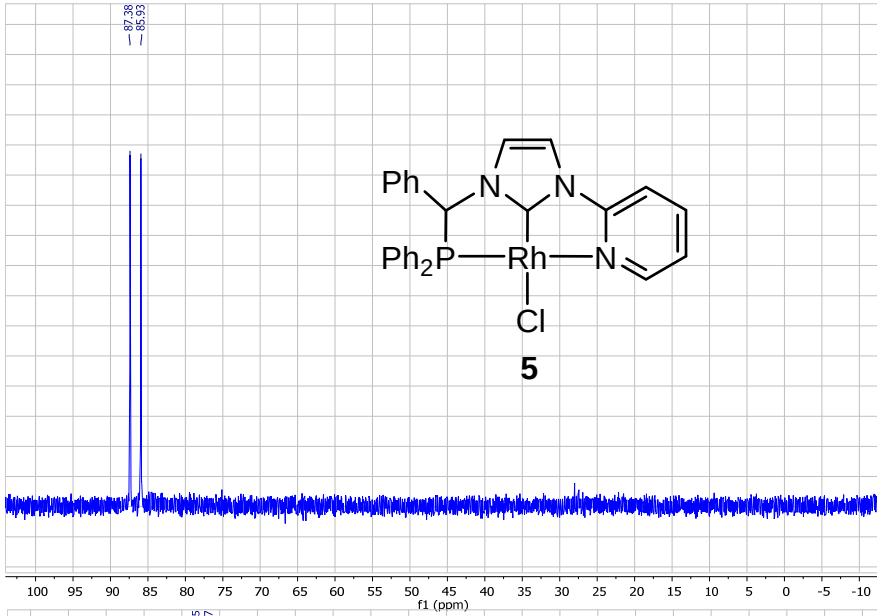


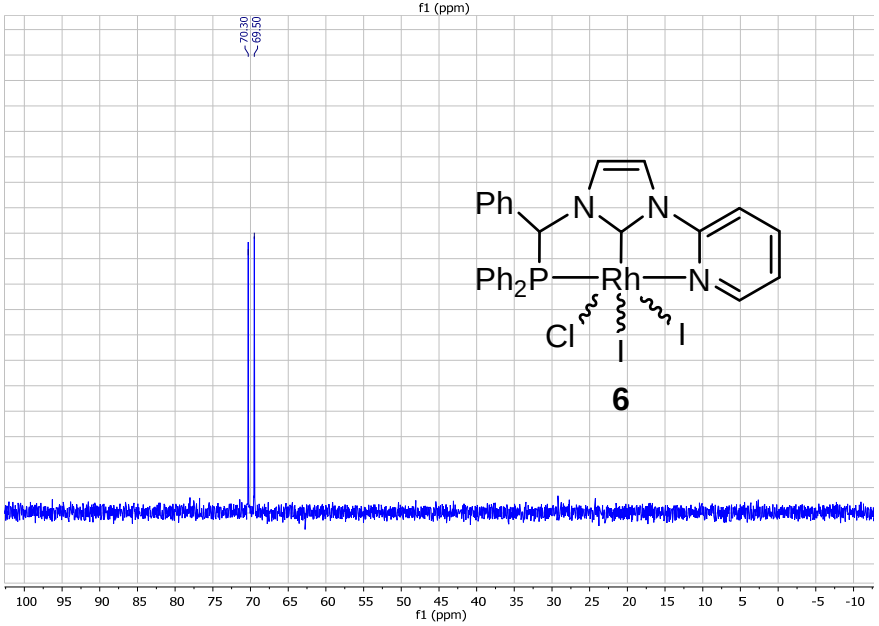


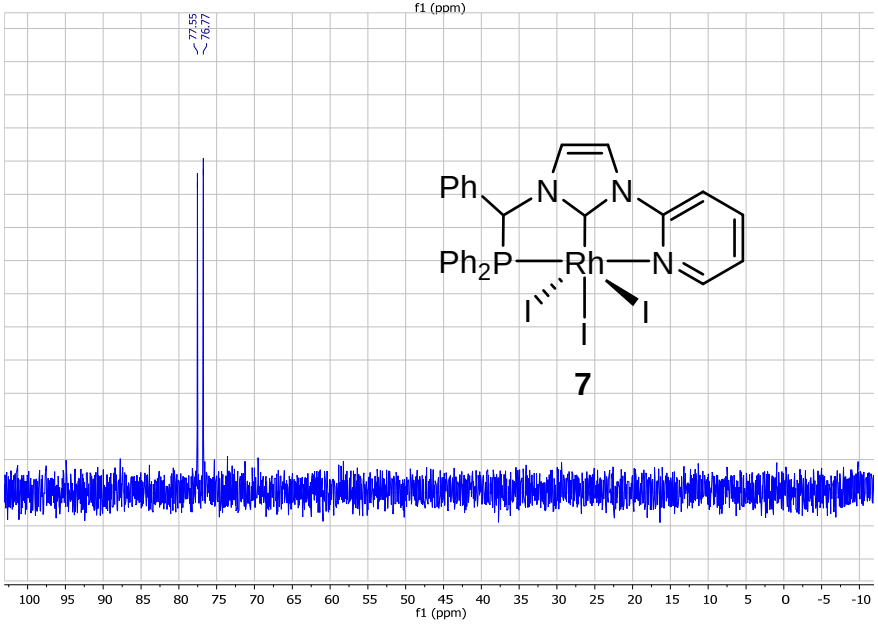

**Figure S18**. $^{1}$H NMR spectrum of complex **7** (400.1 MHz, THF-$d_8$, 25°C), the peaks of residual toluene and water are marked with asterisk

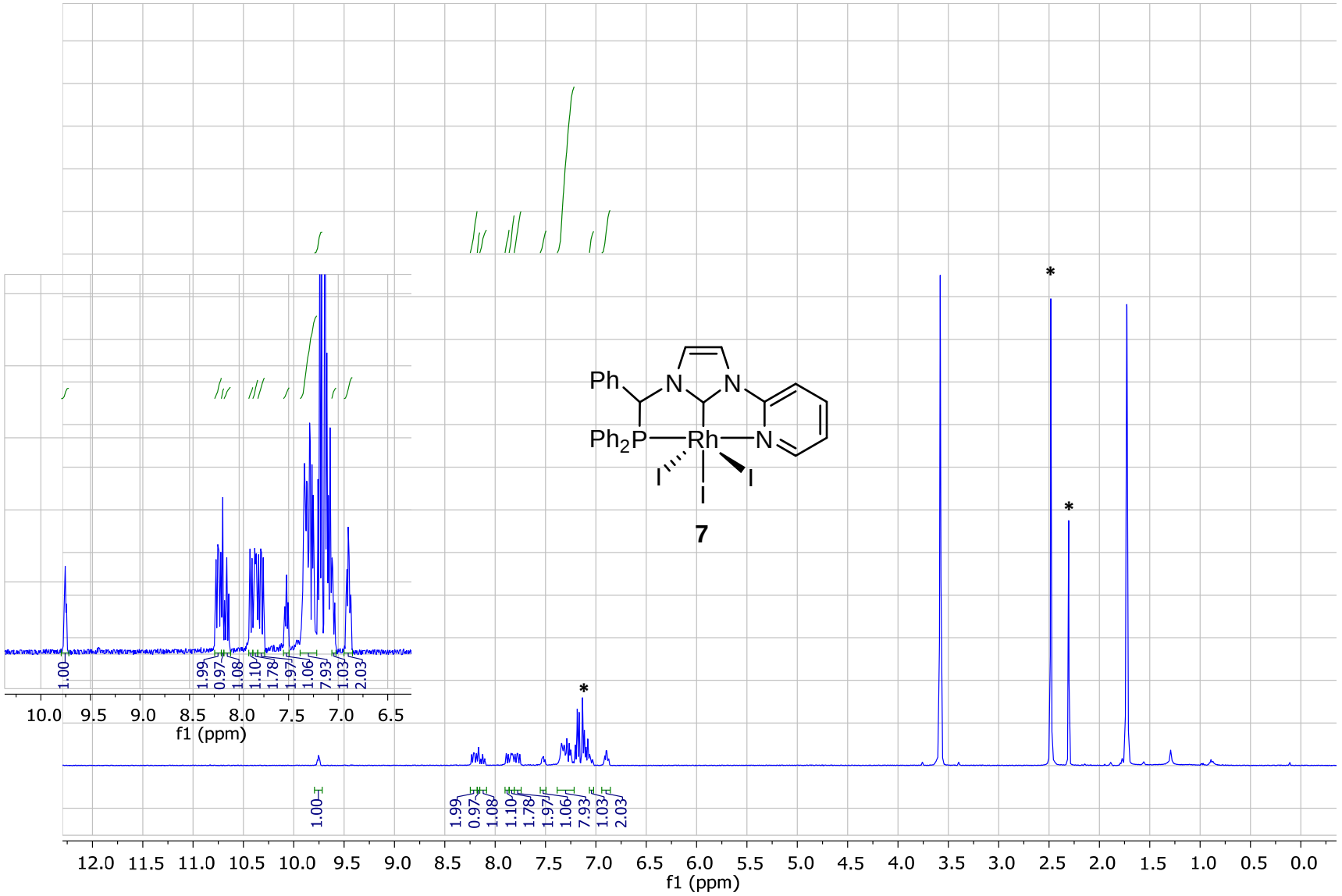

**Figure S19**. $^{1}$H NMR spectrum of complex **7** (400.1 MHz, dmso-$d_6$, 25°C), the peaks of residual water is marked with asterisk

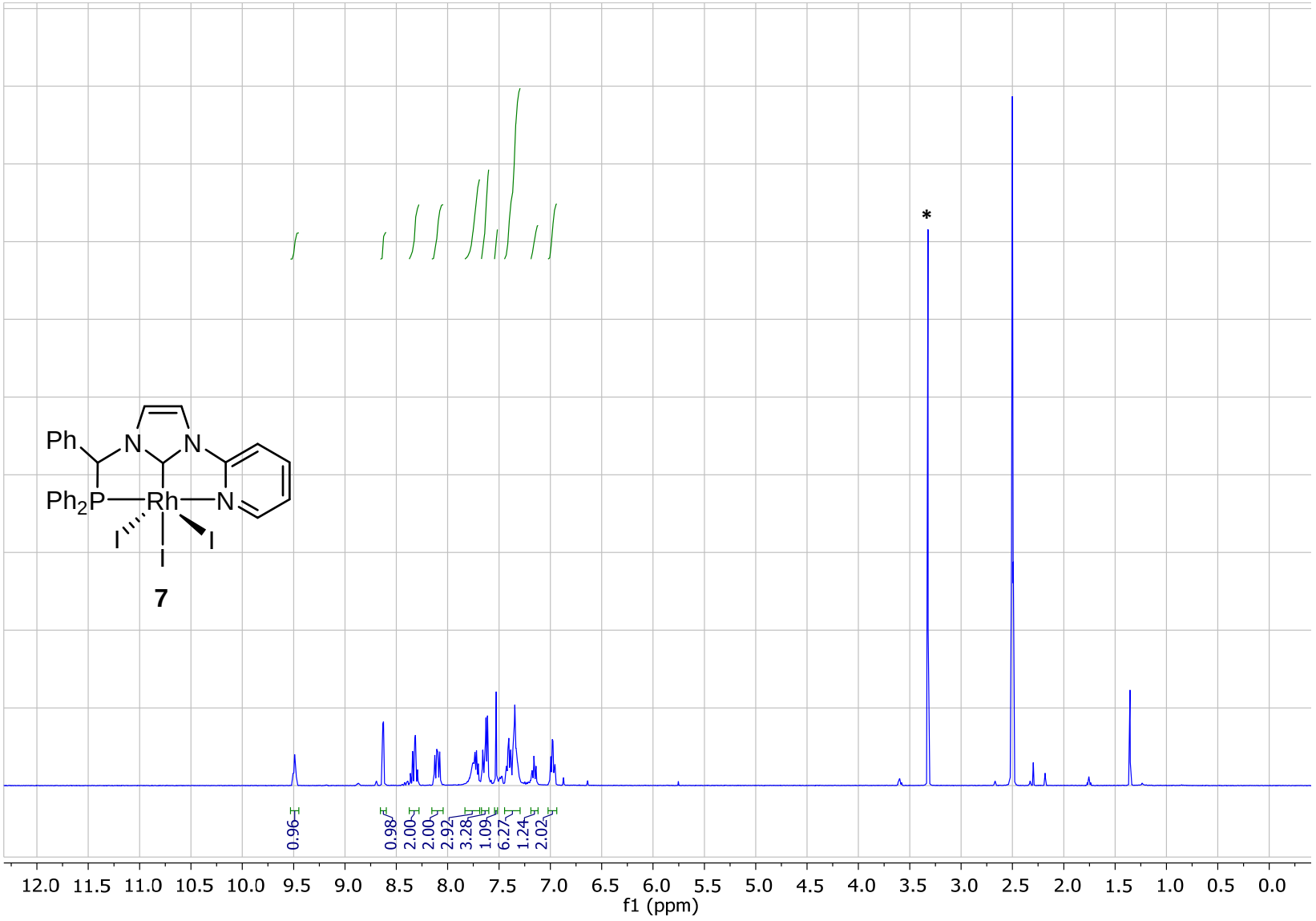

**Figure S20**. $^{31}P\{^{1}H\}$ NMR spectrum of complex **7** (162.0 MHz, THF-$d_8$, 25°C)

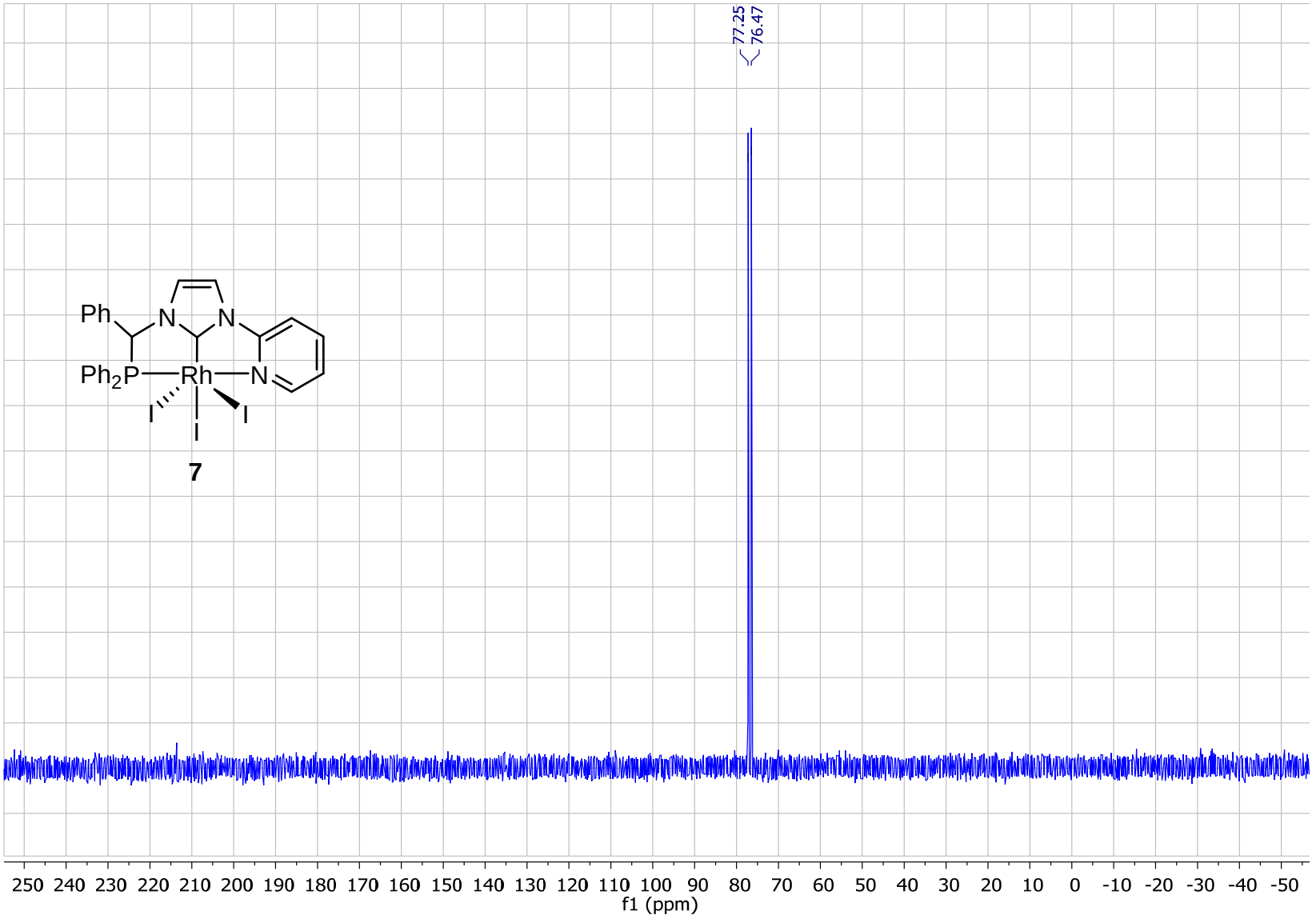

**Figure S21**. $^{31}P\{^{1}H\}$ NMR spectrum of complex **7** (162.0 MHz, dmso-$d_6$, 25°C)

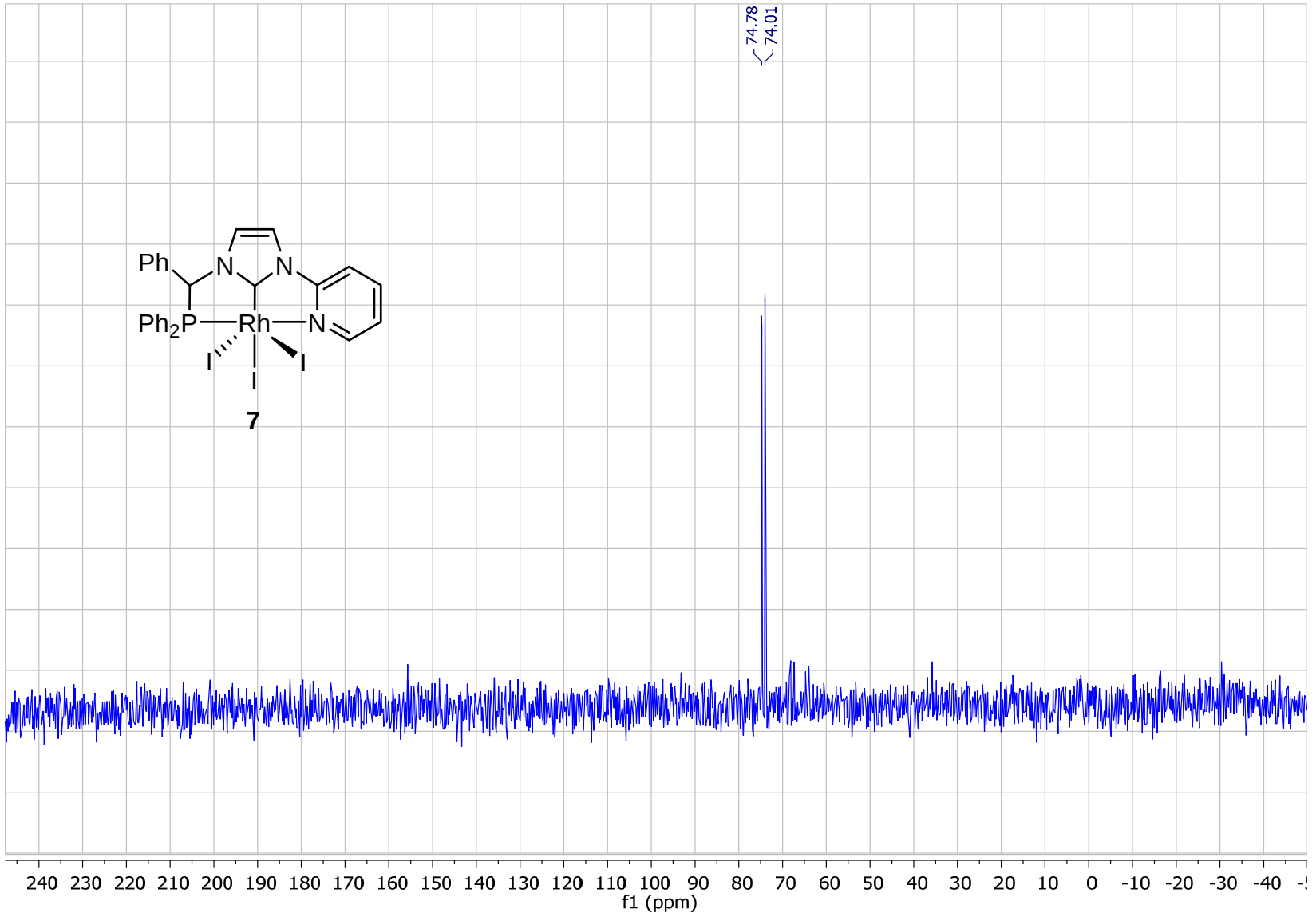

**Figure S22**. $^{13}C\{^{1}H\}$ JMOD NMR spectrum of complex **7** (100.6 MHz, dmso-$d_6$, 25 °C) (CH down, C up)

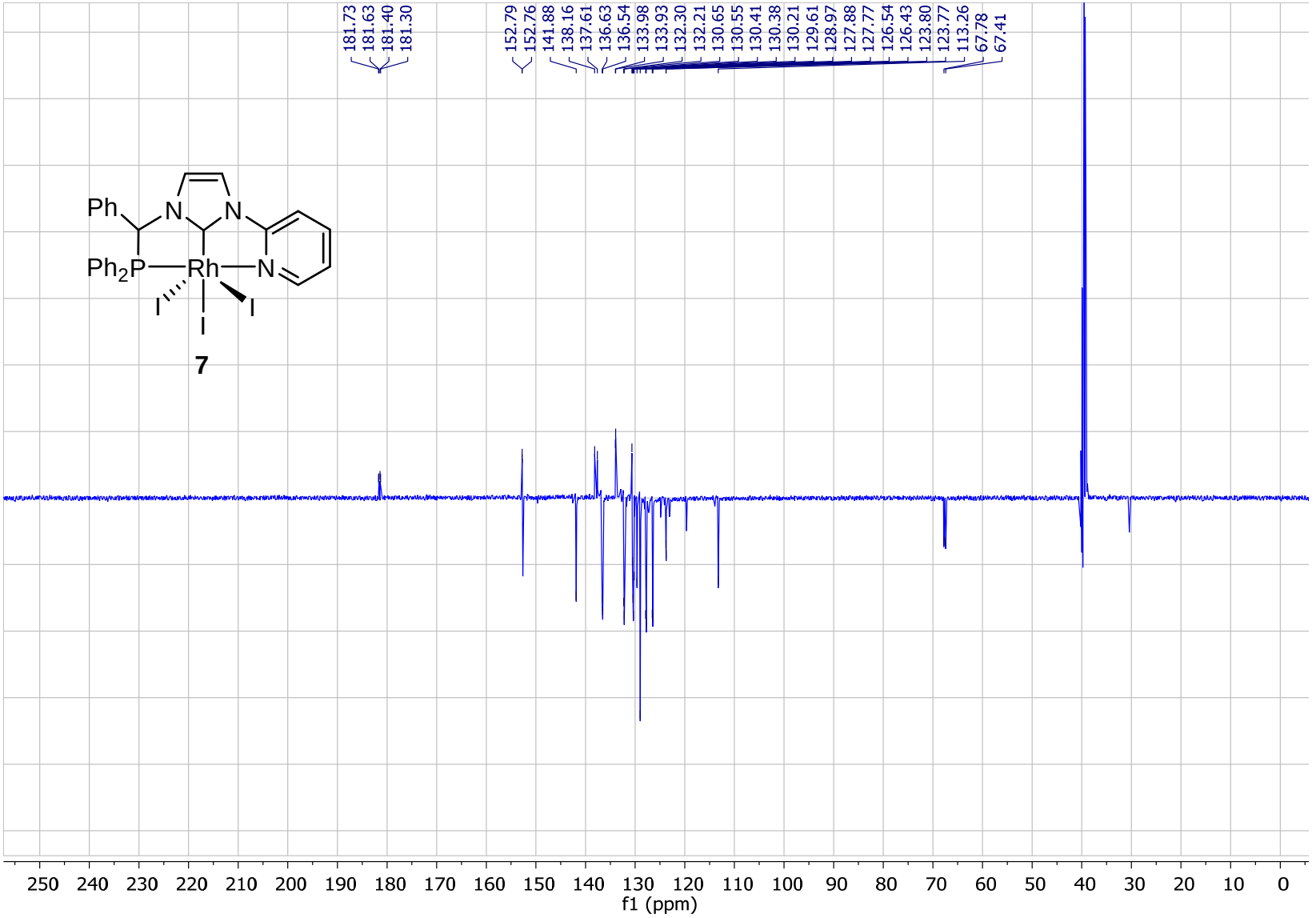

**Figure S23**. $^{13}C\{^{1}H, ^{31}P\}$ NMR spectrum of complex **7** (100.6 MHz, dmso-$d_6$, 25 °C)

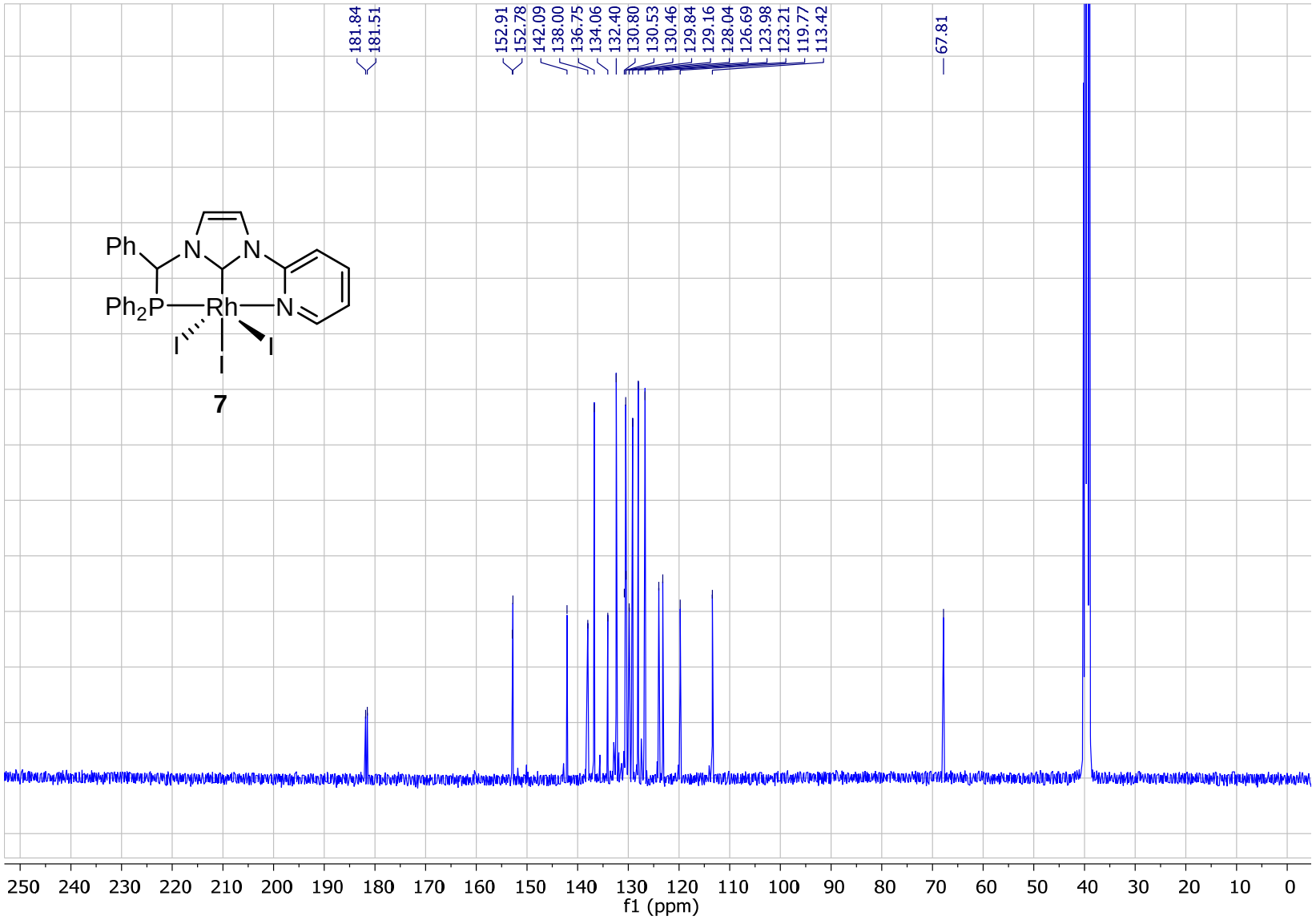

**Figure S24**. $^{1}$H NMR spectrum of complex **8** (500.3 MHz, dmso-$d_6$, 25 °C), signal of water is marked with asterisk

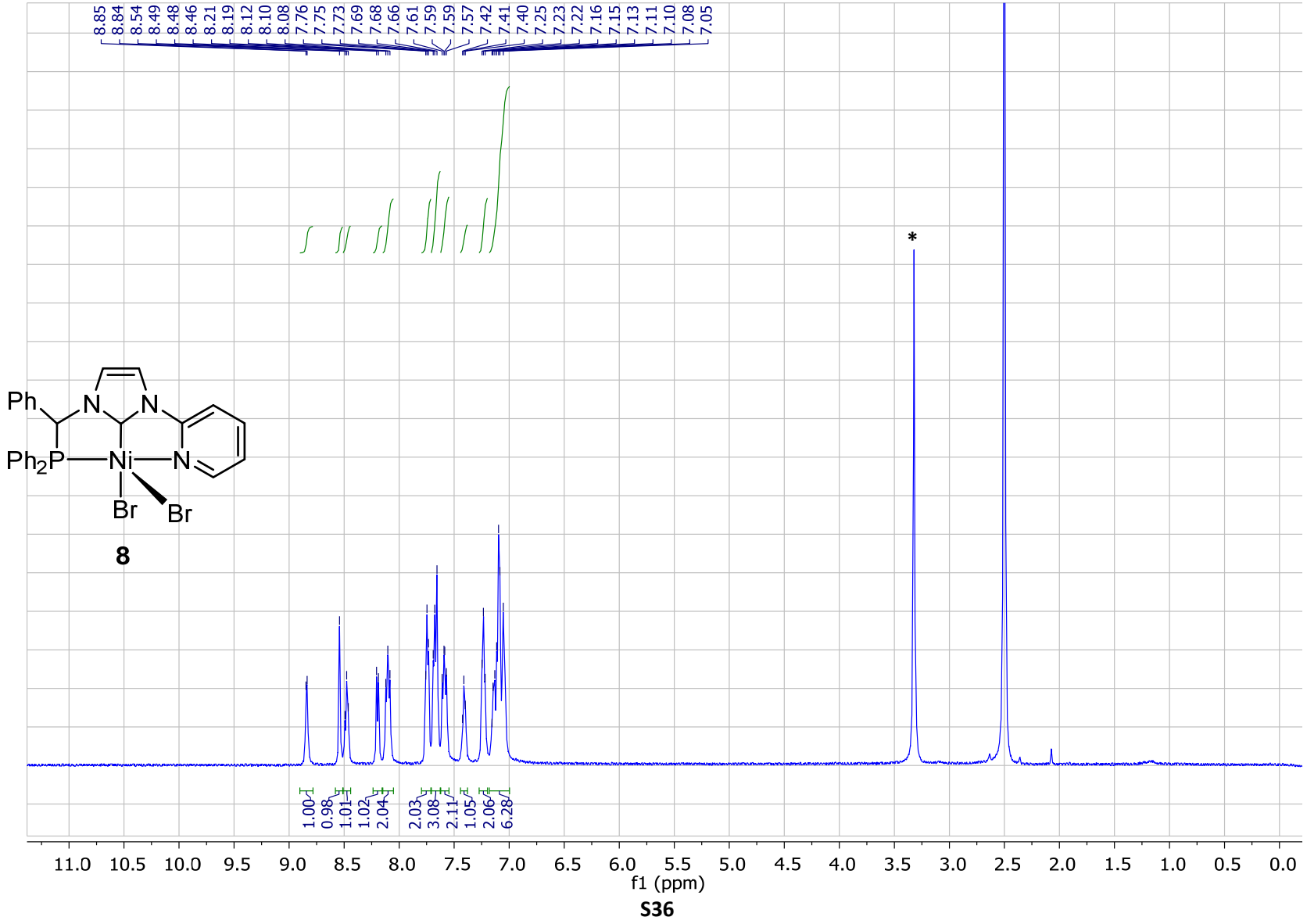

**Figure S25**. $^{31}P\{^{1}H\}$ NMR spectrum of complex **8** (202.5 MHz, dmso-$d_6$, 25 °C)

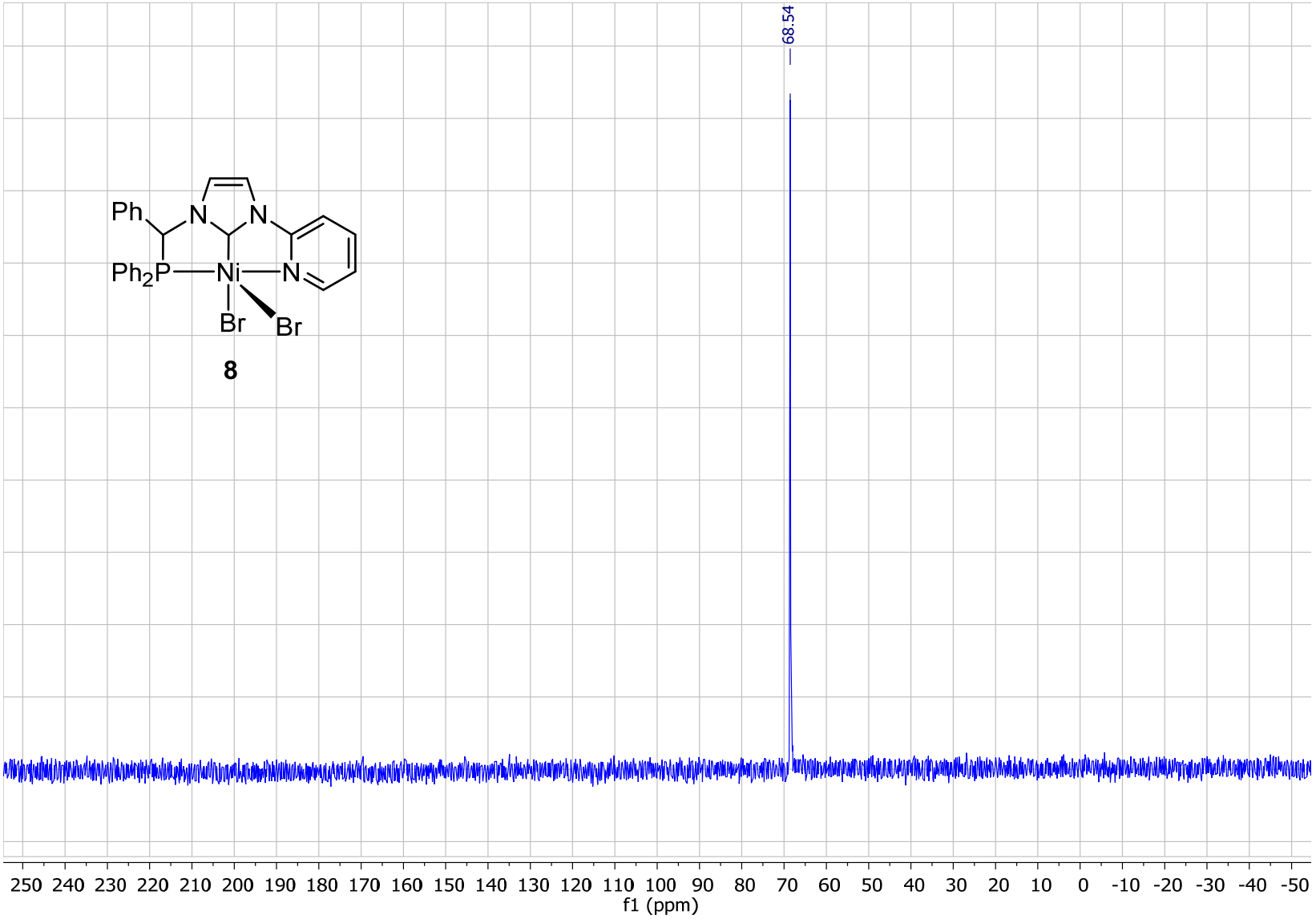

**Figure S26**. $^{13}C\{^{1}H\}$ NMR spectrum of complex **8** (125.8 MHz, dmso-$d_6$, 25 °C)